Abstract

CAI, FANG. Photostability of Surface Bound Dyes. (Under the direction of Dr. Stephen Michielsen.)

The use of photo-generated singlet oxygen has gained considerable attention in the last several years. In this study, the photostability of singlet oxygen generating dyes, Rose Bengal and Azure A, were studied. Both solution and fabric based systems were studied. UV/Vis, FTIR and color test were used to characterize the performance of both dyes. By comparing the performance of one dye in different systems and both dyes in the same system, the durability of dyes under illumination were analyzed. It was found that Rose Bengal behaved similarly in solution and when bound to a fabric surface. In both systems it keeps a gradual decreasing rate; 46% of the original amount of Rose Bengal was left after 8 hours UV exposure in the aqueous system and a 22% drop in the first hour of fabric system. However, Azure A behaves totally differently in aqueous and fabric systems. It is very reactive and unstable in the aqueous system but more stable in fabric system. 18% remained in the aqueous system after 16 hours observation but 56% was found in the fabric system. The comparison between Azure A and Rose Bengal indicates that Rose Bengal is more consistent in aqueous system and Azure A is more stable in the fabric system. The simple linear models of relationship between absorbance and singlet oxygen generating rate parameter obtained in this study make the future work easier.

Photostability of Surface Bound Dyes

by
Fang Cai

A thesis submitted to the Graduate Faculty of
North Carolina State University
in partial fulfillment of the
requirements for the degree of
Master of Science

Textile Engineering

Raleigh, North Carolina

2011

APPROVED BY:

_____	_____
Dr. Stephen Michielsen	Dr. David Hinks
Committee Chair	
_____	_____
Dr. Renzo Shamey	Dr. Kim Weems

Biography

Fang Cai was born on March 20th, 1987, in a small town of Hunan province in China. She attended No.1 Middle School of Hanshou, Hunan for 3 years and got the admission of Donghua University in September, 2005. Since the second year in Donghua University, she worked in Professor Yiping Qiu's lab. In June 2009, she got her Bachelor of Science degree in Nonwoven Materials and Engineering. After that, Fang was accepted to the College of Textiles of North Carolina State University and she got the research assistant scholarship in fall 2009. Then she worked with Professor Stephen Michielsen on solar water purification. After completion of this program and getting her Master's degree, she will begin her career life in textile related field.

Acknowledgements

With many people's help, this research was made possible. I would like to thank both LAAMScience and Textile Engineering, Chemistry and Science department for offering me with this wonderful opportunity to further my education in textile field. I would also like to thank all committee members. My advisor and chair, Professor Stephen Michielsen, guided with his knowledge and experience throughout the entire process and is greatly appreciated. I will keep every suggestion he provided me in my mind because that is great wealth for my rest life. I will never forget those encouragements he gave me in my darkest time. I will be always inspired by his humor, wisdom and honesty. Several others also contributed to this research as well.

I thank my parents and sister; they are all proud of me. They encouraged me on every detail. My boyfriend is also a huge moral support for me. He persuaded me trying to keep positive and took care of my daily life. I could not survive from such a severe challenge without his help.

Table of Contents

List of Schemes

List of Tables

List of Figures

1. Introduction

Over three billion people in the world do not have adequate, clean water. Water purification is always a large challenge. From simple filtering and heating purification systems to chemical purification methods, water purification requires considerable effort. For areas with ample sunlight, but few other resources, solar water purification could provide substantial benefits and is the motivation for this thesis. The proposed method for water treatment uses a special colored fabric, which purifies water when exposed to sunlight, and is also used to filter water. When the fabric is exposed to sunlight, dye attached on the fabric surface produces singlet oxygen, which kills bacteria in the water. In this process there are several challenges. The first challenge is attaching more than one type of dye to the fabric surface. The current fabric is coated by only one dye which uses a specific, narrow region of the spectrum of sunlight. In order to increase the amount of the spectrum used, it would be beneficial to be able to attach more than one type of dye. Another challenge is that dyes tend to degrade over time when exposed to sunshine; however, many places are so remote that it should last several years to simplify maintenance; i.e. they should be photostable.

For this study, Azure A and Rose Bengal were selected because they: 1. can be easily attached to polymers; 2. have high singlet oxygen quantum yield; and 3. are water soluble. In addition, nylon spunbonded fabric was used as the base fabric because it is easy to modify the fiber surface.

The following chapters describe studies of the photostability of these two dyes and their ability to produce singlet oxygen. Chapter two contains a literature review that introduces the

principles of this project and each issue which is related to the reaction system. The literature review also reviews the dyes used in this study and other methods of producing singlet oxygen, which is the key factor in this study. Chapter Three describes the experimental procedures used including both solution and fabric tests. Ultraviolet/visible sprectroscopy (UV/Vis), Fourier transform infrared sprectroscopy (FTIR), and singlet oxygen generation tests are described. The results and discussion are presented in Chapter Four. The test results are analyzed and trendline analyses are presented. Linear and exponential models are used to explain the relationships between pairs of factors. Comparisons are made either in the same system for different dyes or in different systems for the same dye. Finally, Chapter Five provides the conclusions and Chapter Six suggests additional future work recommendations.

Rose Bengal and Azure A were found to perform differently in different systems. And the linear model is very meaningful for the future testing work because it simplifies the test.

2. Literature Review

In this chapter, a brief review of the singlet oxygen, its production, and some of its are presented. Next, several photocatalysts are presented and photobleaching is discussed. Finally, the attachment of photocatalysts to the surface of fibers using grafting is reviewed.

2.1 Introduction of singlet oxygen

Molecular oxygen, O_2, is a unique and fascinating molecule that is integral to many processes that occur on earth {{26 Lane, N. 2002}}. It plays a key role in the maintenance of life, and in mechanisms by which life is extinguished and materials destroyed. Despite its acknowledged significance, the study of oxygen and oxygen-dependent processes continues to present many challenging problems. The properties and behavior of oxygen are both tightly related to its unique electronic structure. It has two unpaired electrons in its lowest energy state, which is a triplet state. The lowest two excited states are both spin singlets and confer high chemical reactivity. Although the higher energy state is not known to react with other molecules, the lower energy state has a rich chemistry that is very different from that of the ground triplet state in solution phase systems. This lowest excited singlet state is commonly called "singlet molecular oxygen" or ''singlet oxygen,'' ($^1O_2$).

Singlet oxygen has been studied for more than 80 years since Milliken proposed its existence in 1928 {{27 Milliken, R.S. 1928}}. By the early 1950s, a great deal had been learned about the gas phase spectroscopy of singlet oxygen {{29 Herzberg, G.}}. In the early 1960s, many papers were published that confirmed Kautsky's hypothesis that singlet oxygen was indeed involved in solution-phase photosensitized oxygenation reactions {{30 Foote, C. S.

1964}}.The latter research on singlet oxygen transferred to the development and application of techniques by which solvated singlet oxygen could be directly monitored in both steady state and time-resolved optical experiments {{31 Krasnovsky, A. A. 1979}}. Since then, further developments in the spectroscopic detection of singlet oxygen, particularly in biological systems, have continued to stimulate new activities.

2.2 Production of singlet oxygen

Singlet oxygen ($^1O_2$) is generated by many different types of reactions. The following scheme shows 12 detail methods of producing singlet oxygen from photochemical, chemical and biological systems separately. Among them, the photochemical system shown as in Scheme 2.1 is the one most frequently used in research and industry.

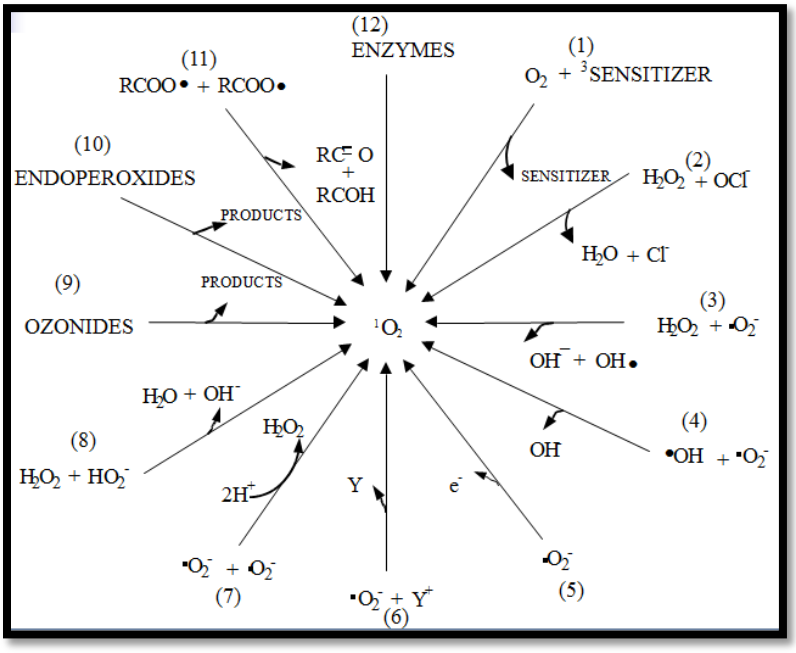

Scheme 2.1: Singlet oxygen sources [wikipedia]

2.2.1 Photochemical system

In this reaction system, there is a light activated process that requires the presence of a light absorbing substance, the photosensitizer, that initiate a physical, chemical, or biological process in a non absorbing substrate. The production of $^1O_2$ by a photosensitizer involves four steps {{32 B. W. Henderson 1992}}: 1. absorption of light by the photosensitizer; 2. formation of the photosensitizer's triplet state; 3. trapping of the triplet state by molecular oxygen within its lifetime; and 4. energy transfer from the triplet state of the dye to molecular oxygen. The basic scheme of this reaction is represented in Scheme 2.2.

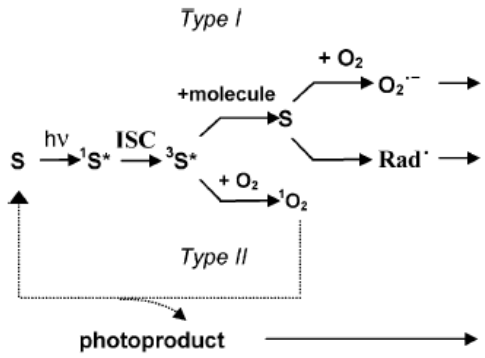

Scheme 2.2: Possible mechanisms of photodynamic therapy (PDT) effect {{32 B. W. Henderson 1992}}

Following the absorption of light, the sensitizer undergoes a transition from its ground state (S) into an electronically excited state (singlet $^1S^*$) and from there to an excited triplet $^3S^*$ state via intersystem crossing. Different reactions can take place from here on, but the triplet state mainly undergoes two kinds of reactions: it can form radicals ($O_2^{\bullet-}$, $Rad^{\bullet}$) after directly reacting with the substrate by hydrogen atom or electron transfer (Type I mechanism), or it

can transfer its energy to molecular oxygen by directly reacting to form singlet oxygen ($^1O_2$, Type II mechanism). Type I and II reactions may occur simultaneously, and the ratio between the two processes depends on the sensitizer, substrate and oxygen concentration.

2.2.2 Chemical system

Chemical systems provide another important path to generate singlet oxygen. Spectroscopic and chemical evidence demonstrate singlet oxygen formation during the reaction of H_2O_2 with acetonitrile in alkaline solution {{33 Eduardo A. Almeida 2003}}. According to the mechanism proposed by Wiberg in 1953 for singlet oxygen production, we can expect first a nucleophilic attack by the peroxide anion ($^-$OOH) on the carbon of the nitrile (Scheme 2.3 A). A reaction with a second molecule of H_2O_2 generates acetamide, water and $^1O_2$ (Scheme 2.3 B). Together, these novel observations serve as important evidence of $^1O_2$ production in the reaction of H_2O_2 and acetonitrile in alkaline solution.

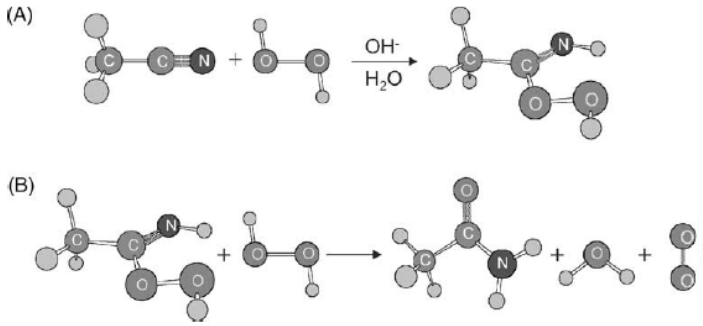

Sheme 2.3: Reaction of acetonitrile with hydrogen peroxide in alkaline media generating acetamide, water and singlet molecular oxygen {{33 Eduardo A. Almeida 2003}}

Other reactions such as peroxynitrite with hydrogen peroxide and hypochlorite with hydrogen peroxide were studied as well {{34 Paolo Di Mascio 1994}}{{35 Alice Maetzke 2006}}. They are based on the same principle as the acetonitrile reaction.

2.2.3 Biological system

Singlet oxygen production has been demonstrated in several model enzymatic systems. More importantly, a living cell, the human eosinophil, has been shown to produce modest amounts of singlet oxygen. The biochemical production of singlet oxygen has been proposed to cause the destructive effects existing in many biological processes. Several model biochemical systems have been found to produce singlet oxygen {{36 M. Anbar 1966}}. These systems include the peroxidase-catalyzed oxidations of halide ions, the perosidase-catalyzed oxidations of indole-3-acetic acid, the lipoxygenase-catalyzed oxidation of unsaturated long chain fatty acids and the bleomycin-catalyzed decomposition of hydroperoxides.

2.2.3.1 Peroxidase-hydrogen-peroxide-halide system

In 1972, Allen et al. proposed that polymorphonuclear leukocytes generate singlet oxygen by a perxidase-dependent mechanism,

$$H_2O_2 + X^- \xrightarrow{\text{peroxidase}} HOX + OH^-$$
$$H_2O_2 + HOX \longrightarrow H_2O + X^- + {}^1O_2$$

where X is a halide ion {{38 R.C. Allen 1972}}. Reaction 2 is known to efficiently generate singlet oxygen, when X is either a chloride ion or bromide ion and myeloperoxidase can

oxidize chloride ion to hypochlorous acid.

2.2.3.2 Dismutation of superoxide anion

The production of excited oxygen species from the recombination of peroxyl radicals including $HO_2^{\cdot}$ was first suggested by Stauff et al. {{39 J.E. Baldwin 1986}}. Khan subsequently proposed that singlet oxygen was a product of the dismutation of superoxide anion {{40 A.U. Khan 1970}}

$$HO_2\bullet + O_2^- \longrightarrow HO_2^- + {}^1O_2$$

This process could explain the disparity between the relatively low chemical reactivity of superoxide ion in aqueous solutions and its potent toxic effects in biological systems.

2.2.3.3 Lipoxygenase

Lipoxygenases are a class of enzymes which catalyze the oxidation of long chain unsaturated fatty acids. Singlet oxygen is produced from the reaction of peroxyl radicals through a Russell mechanism {{41 T. Matsuura 1969}},

$$2RR'HCO_2\bullet \longrightarrow RR'CO + RR'CHOH + {}^1O_2$$

Under optimal conditions, soybean lipoxygenase-2 could produce 12% of the singlet oxygen predicted by this Russell mechanism. Soybean lipoxygenase-1 could produce singlet oxygen only at low oxygen concentrations {{42 R.M. Howes 1971}}.

2.3 Application of singlet oxygen

After $^1O_2$ is generated, it can either lose its energy through a radiative process, a non-radiative process, i.e. heat, or it can react with a substrate. The reactivity of singlet oxygen can be detrimental, as is the case in the photodegradation of polymers, but can also be beneficial as is illustrated in this section.

2.3.1 Waste water treatment

The use of singlet oxygen in the synthesis of fine chemicals and in the treatment of wastewater is more and more interesting to researchers. It is a useful synthetic reagent because of its versatility and the high degree of stereo selectivity. The use of solar energy in the treatment of wastewater may be an economical solution to a difficult environmental problem. Research into photosensitized detoxification and treatment of industrial and urban waste-waters using light concentrated directly from the sun is being carried out in a Spanish project -- the Plataforma Solar de Almeria (PSA) {{43 P. Esser 1994}}. Likewise, work has begun at PSA on project 'SOLFIN' and at the PROPHIS {{44 P. Wagler, B. Heller, O. Orther, K.H. Funkn, G. Oehme 1996}} reactor in Germany, both applied to photosensitized fine chemical synthesis. For example, work from PSA has verified the synthesis of 5-hydroxy-5H-furan-2-one from furfural in the presence of methylene blue or Rose Bengal photosensitizers in ethanol {{43 P. Esser 1994}}.

2.3.2 Photodynamic processes

The photodynamic effect describes the damage of living tissue by the combination of a photosensitizer, visible light, and oxygen. Singlet oxygen plays the major role in this effect, and application of this effect to blood sterilization, cancer therapy, insecticides and herbicides is increasingly important. Direct spectroscopic evidence of singlet oxygen in photodynamic therapy (PDT) is difficult to find, maybe due to the rapid reaction of singlet oxygen with biomolecules. However, it is generally agreed that $^1O_2$ is the major participant.

2.3.2.1 Blood sterilization

The Swiss and German Red Cross use methylene blue as a photosensitizer for the decontamination of freshly frozen plasma units {{45 W.M. Sharman, G.M. Allen, J.E. VanLier, 1999}}. Because of its non-toxicity to humans, the dye is effective at destroying extracellular enveloped viruses. However, cellular enzymes reduce this dye to a photodynamically inactive colorless form, thus limiting its use as a photosensitizer in this application.

2.3.2.2 Photodynamic therapy (PDT) of cancer

Photodynamic therapy for the treatment of cancer is gaining research interest due to the possibility of selectivity for diseased tissue. In PDT, visible light, a light-sensitive drug (photosensitizer), and oxygen are combined together to lead to the production of lethal agents to inactivate tumor cells. It is accepted that singlet oxygen is the major cytotoxic agent

contributing photobiological activity {{46 R. Bonnett 1995}}. The dual selectivity of PDT which comes from both the localization of the sensitizer in the tumor and the ability to confine activation of the photosensitizer by illumination of only the tumor region allows for the possibility of tumor destruction without affecting on normal tissue which is a major goal in cancer therapy.

The process of PDT is as follows {{46 R. Bonnett 1995}}: the photosensitizer is administered (orally, topically, or intravenously) and the drug equilibrates for a certain period of time (drug-light interval), to achieve maximum tumor/normal tissue differentiation. The tumor is then irradiated directly by a light source with the proper wavelength. Lasers and fiber optics are often used as the light source, but a simple projector lamp can be used as well. Finally, cytotoxic products generated by the excited photosensitizer cause the expected tumor destruction, preferably without consequence on other normal healthy tissues.

2.3.3 Insecticides and herbicides

Like the work done in the PDT of cancer, photodynamic herbicides and insecticides use the toxic effects of singlet oxygen to destroy undesired plants and pests. Photodynamic herbicides cause the undesirable accumulation of chlorophyll and heme metabolic intermediates, tetrapyrroles, in green plants {{47 C.A. Rebeiz, K.N. Reddy, O.B. Nadihalli, J. Velu, J 1990}}. Once exposed to light, these accumulated tetrapyrroles act as photosensitizers for the production of singlet oxygen, which kills the treated plants through oxidation of their tissues. These tetrapyrrole-dependent photodynamic herbicides (TDPH)

generally consist of d-aminolevulinic acid (ALA), which is a precursor of all tetrapyrroles in plant and animal cells and modulators, which can change the tetrapyrrole accumulation.

2.4 Photosensitizers

$^1O_2$ can be produced via gaseous discharge or chemical reactions {{48 Schultz 1885}}. However, large varieties of practical applications, especially in medicine, require its generation in organic solvents or human tissue in a controlled manner. Therefore, the most common $^1O_2$ generation procedure contains photosensitizers. There are several groups of UV/visible absorbing molecules that have shown singlet oxygen generating ability. Photosensitizers should have the following properties: (1) high absorption coefficient in the spectral region of the excitation light; (2) a triplet state of appropriate energy (>95 kJ/mol) to allow for efficient energy transfer to ground state oxygen; (3) high quantum yield of the triplet state (>0.4) and long triplet state lifetimes (>1 μs), since the efficiency of the photosensitizer is dependent on the photophysical properties of its lowest excited triplet state; and (4) high photostability.

2.4.1 Organic dyes

Dyes such as Rose Bengal, eosin, and methylene blue are very effective photosensitizers, as they possess triplet states of appropriate energies for sensitization of oxygen. Methylene blue is a phenothiazinium dye with a strong absorbance in the range of 550-700 nm, and a relatively high quantum yield (ϕ=0.52) {{50 S. N. Gupta, S. M. Linden, A. Wrzyszczynski

and D. C. Neckers, 1988}}. Xanthene dyes such as Rose Bengal and eosin show intense absorption bands in the green area of the visible spectrum (480-550 nm) and produce singlet oxygen with high yields. Rose Bengal for example has a quantum yield equals 0.76 {{50 S. N. Gupta, S. M. Linden, A. Wrzyszczynski and D. C. Neckers, 1988}}.

2.4.1.1 Rose Bengal

Rose Bengal, 2,4,5,7-tetraiodo-3',4',5',6'-tetrachlorofluorescein, was originally synthesized by Gnehm {{48 Schultz 1885}}as a fabric dye to mimic the red colors in "Bengalis". Its name is connected to the red symbolic spot worn at the part of the hair by Bengali women to symbolize marriage. Rose Bengal, sodium salt, and its derivatives are widely used for its special spectral, photophysical, and photochemical properties. The synthesis of the xanthenes is from resorcinol and a phthalic anhydride, in the case of Rose Bengal tetrachlorophthalic anhydride {{78 D. C. NECKERS 1989}} (Scheme 2.4).

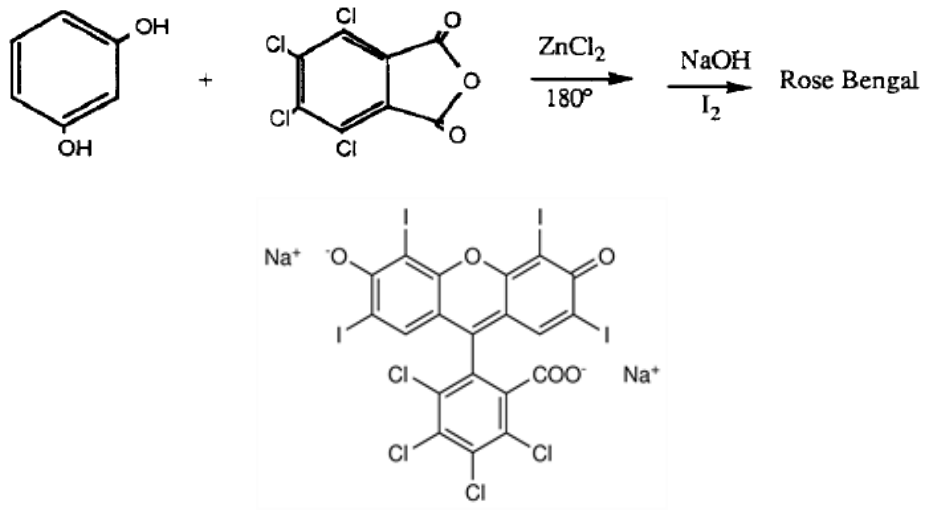

Scheme 2.4: Synthesis of Rose Bengal and chemical structure of Rose Bengal

According to Jodlbauer and von Tappeiner {{51 A. Jodlbauer, H. von Tappeiner 1905}}, the triplet state of Rose Bengal, disodium salt, is “completely quenched” by oxygen in polar solvents producing singlet oxygen and superoxide radical ion. It is this property more than any other which was responsible for the wide scale use of Rose Bengal in the first place. Rate constants for oxygen quenching are at the diffusion-controlled limit under conditions of air saturation in all solvents.

Singlet oxygen yields for several monomeric derivatives of Rose Bengal have been measured by previous researchers. Because Rose Bengal, disodium salt, is only soluble in polar solvents, certain of the oxidation products formed in singlet oxygen reactions may be consumed by these solvents in secondary reactions. For singlet oxygen quantum yields from those Rose Bengal derivatives which have been reported, in polar solvents the values for each of the compounds do not vary much {{78 D. C. Neckers 1989}}.

Superoxide radical anion ($O_2 \cdot^-$) was first reported formed from Rose Bengal by Srinivasan et al. {{52 V. S. Srinivasan, D. Podolski, N. Westrick, D. C. Neckers, 1978}}. In a clever experiment $O_2 \cdot^-$ was detected with superoxide dismutase and an oxygen electrode in water in the presence of sulfite. This result was confirmed quantitatively in water where 25% superoxide was observed {{53 M. A. J. Rodgers, P. Lee 1984}}. Superoxide formation may require something other than direct electron transfer from Rose Bengal triplet. The energetics allow self-quenching electron transfer followed by electron transfer from the radical anion of Rose Bengal to dioxygen. However, the mechanism is bimolecular in Rose Bengal and

suggests that the $O_2 \cdot^-$ yield should increase with the concentration of the dye. Though there is no related literature on the yield of superoxide as a function of Rose Bengal concentration so far.

2.4.1.2 Azure A

Like Rose Bengal, because of its photophysical properties, methylene blue (MB) is frequently used as a photosensitizer in light induced reactions. These studies are important particularly from the point of the possibility of their utilization in photodynamic therapy (PDT), photodegradation of environmental contaminants, molecular recognition and photosensitized modification of DNA. But thiazine dyes (Scheme 2.5) named as azures are possible photosensitizers for PDT {{54 Martina HavelcovaÂ , Pavel KubaÂ t , Irena NeÏmcovaÂ 2000}}, and are more stable in aqueous solutions as they do not undergo demethylation {{54 Martina HavelcovaÂ , Pavel KubaÂ t , Irena NeÏmcovaÂ 2000}}, in contrast to MB.

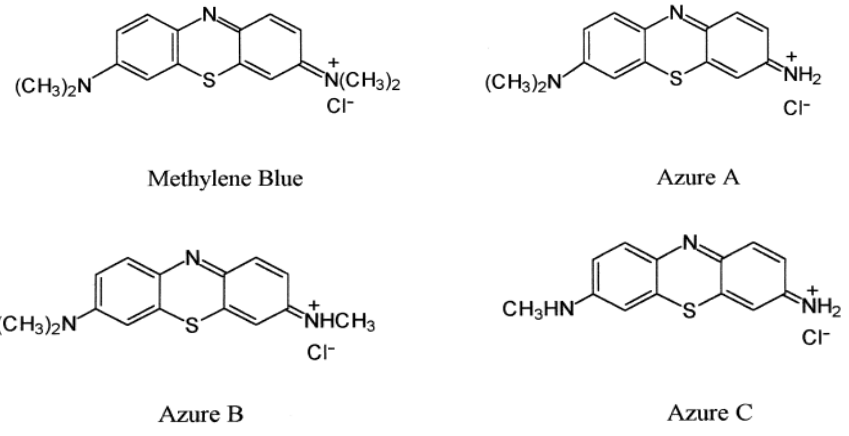

Scheme 2.5: Chemical structures of MB and azure dyes

During the excitation of azure A (AA), protonated and unprotonated triplet states are formed, along with the radical cation $AA^{2+\bullet}$. $^3AA^+$ is quenched by oxygen with the formation of $^1O_2$. The mechanism of formation of the radical cation following laser excitation has been studied {{54 Martina HavelcovaÂ , Pavel KubaÂ t, Irena NeÏmcovaÂ 2000}}. Several mechanisms have been suggested for its formation, including loss of an electron from the triplet state in neutral or acidic medium [Equation a] and interaction of O_2 in the ground state with the triplet state of the dye, with formation of a superoxide anion [Equation b].

$$^3AA \rightarrow AA^{+\bullet} + e^-(aq) \qquad (a)$$

$$^3AA + {}^3O_2 \rightarrow AA^{+g} + O_2^- \qquad (b)$$

It is also indicated that in neutral medium (pH 7) {{54 Martina HavelcovaÂ , Pavel KubaÂ t, Irena NeÏmcovaÂ 2000}}, the dyes AA, AB and AC generate singlet oxygen with high quantum yield, comparable with MB within experimental error; therefore these substances can be used as sensitizers for photochemical and photobiological applications.

The degradation of Azure A dye is another application based on its photochemical properties. Photocatalysis is a process by which a semiconducting material absorbs light of energy more than or equal to its band gap, thereby generating holes and electrons, which can further generate free-radicals in the system to oxidize the substrate. The resulting free-radicals are very efficient oxidizers of organic matter. A detailed analysis of electronic and charge–transfer processes occurring during heterogeneous photocatalysis onTiO_2 has been

summarized in reviews {{55 T. Aarthi, Prashanthi Narahari, Giridhar Madras 2007}}. In T. Aarthi's research {{55 T. Aarthi, Prashanthi Narahari, Giridhar Madras 2007}}, the photocatalytic degradation of Azure A was investigated with two catalysts. The photocatalytic activity of solution combustion synthesized TiO_2 (CS TiO_2) was compared with that of Degussa P-25 for degrading Azure A and other dyes. It was found that CST and Degussa P-25 were helpful in increasing the degradation rate of Azure A. And when the concentration of the nitrate salt was 200 μM, the presence of metal ions like Cu^{2+}, Al^{3+}, Co^{2+} and Zn^{2+}, reduced the initial rates of photocatalytic degradation of Azure A in the presence of CS TiO_2, by 72, 53, 64 and 62%, respectively. When the concentration of chloride salt was 200 μM, the presence of Cu^{2+}, Co^{2+}, Fe^{3+}, reduced the initial rates of photocatalytic degradation of Azure A by 88, 68 and 42%, respectively.

2.4.2 Porphyrins, phthalocyanines, and related tetrapyrroles

The porphyrins and their derivatives have the ability to absorb several wavelengths in the UV/visible range. The Soret band in the blue and the Q-band in the red are major bands, which represent important components of sunlight. The long-lived triplet states of many porphyrins allow for high quantum yields, and substituents on the macrocycle, metal ions coordinated at its centre, and ligands attached to the axial positions of the metal ion allow for tuning of the porphryins properties. Finally, some porphyrins undergo rapid decomposition in the presence of $^1O_2$ (photobleaching). Apparently, this can be deleterious in some industrial applications; however, it could be an advantage in biological systems where rapid breakdown of the photosensitizer after use is necessary. A well-studied porphyrin used in the

photosensitized production of singlet oxygen is haematoporphyrin {{56 D. Wo¨ hrle, A. Hirth, T. Bogdahn-Rai, G. Schnurpfeil, M. Shopova 1998}}. While its triplet quantum yield and singlet oxygen production quantum yields are high (0.83 and 0.65, respectively), its absorption at 630 nm ($3500 M^{-1}cm^{-1}$) is weaker than the ideal for a photosensitizer {{56 D. Wo¨ hrle, A. Hirth, T. Bogdahn-Rai, G. Schnurpfeil, M. Shopova 1998}}.

2.4.3 Transition metal complexes

Most studies in singlet oxygen photosensitization contain organic molecules. However, some inorganic complexes have also been shown to be efficient photosensitizers. For example, transition metal complexes of ruthenium (II), have relatively strong absorption in the UV/vis regions of the spectrum. Long lifetimes of emission from the triplet metal-to-ligand charge transfer states of many Ru (II) complexes allow oxygen quenching to be an efficient process in aerated solutions. Furthermore, it is thermodynamically possible for many Ru(II) diimine complexes to sensitize oxygen. Many of the ruthenium-based photosensitizers have been found to be more efficient $^1O_2$ producers than the well-studied organic photosensitizer methylene blue, and comparable to the widely used Rose Bengal.

Early work by Demas et al. {{57 J.N. Demas, E.W. Harris, R.P. McBride 1977}} studied the oxygen quenching of 16 luminescent diimine (2,2'-bipyridine,1,10-phenanthroline and/or substituted phenanthroline) metal complexes of Ru(II), Os(II), and Ir(III). This work found quantum yields of singlet oxygen formation of 0.68-0.86 for Ru(II) and Os(II) complexes. Ru(II)tris-bipyridine, $[Ru(bpy)_3]^{2+}$, in particular, was shown to be an effective

photosensitizer of singlet oxygen with a quantum yield of 0.86 in oxygen-saturated methanol at 1 atm.

2.5 Photobleaching

For the organic dyes photosensitizers, there is a big problem to be considered-photostability since they are exposed to light directly. One of the processes that reduces the photostability is photobleaching caused by photochemical reactions that remove molecules from the absorption-emission cycle. Often photobleaching constitutes an undesired effect in various fluorescent-based detection experiments. For example, the use of multiphoton-induced confocal fluorescence microscopy is often limited by increased photobleaching {{58 S. Gavrilyuk,S. Polyutov, P. C. Jha, Z. Rinkevicius, H. Ågren, F. Gel'mukhanov 2007}} due to the decrease of the amount of fluorescence photons and, therefore, the decrease of the sensitivity and accuracy of measurements. Photochemical reactions remove molecules from the absorption-emission cycle.

Previous researchers presented a dynamical theory of multiphoton-induced fluorescence accompanied by photobleaching {{58 S. Gavrilyuk,S. Polyutov, P. C. Jha, Z. Rinkevicius, H. Ågren, F. Gel'mukhanov 2007}}. Their model includes a manifold of singlet and triplet states. The lowest triplet state has a permanent population due to the long lifetime, meaning that the photobleaching occurs mostly from this state and that a quadratic dependence of characteristic bleaching time on light intensity is observed. They obtain simple analytical expressions for the main characteristics of fluorescence accompanied by photobleaching, namely, the photobleaching time. This time depends on the peak intensity, repetition rate,

pulse duration, and microscopic parameters of the single molecule such as the absorption cross section, relaxation rates, and rate of intersystem crossing. There is another potential mechanism of photobleaching of chlorophyll {{59 Robert Livingstos 1947}}:

$$GH + h\gamma \rightarrow GH^* \qquad GH^* \rightarrow GH + h\gamma f$$

$$GH^* \rightarrow HG \qquad HG \rightarrow GH$$

$$HG + BH \rightarrow GH_2 + B \qquad GH_2 + B \rightarrow GH + BH$$

where GH is normal chlorophyll; GH* is electronically excited (singlet state) chlorophyll; HG is long-lived activated chlorophyll (probably in a tautomeric, triplet state); GH_2 is the partly reduced, bleached form of chlorophyll; and BH is a reactive, reducing impurity present in the solvent. This mechanism leads to the following expression for the change in chlorophyll concentrations, ΔC, at steady state.

$$\Delta C = \left[\frac{k_3}{k_2 + k_3} \times \frac{k_5(\mathrm{BH})}{k_4 + k_5(\mathrm{BH})} \times \frac{I}{k_6} \right]^{\frac{1}{2}}$$

This equation indicates that steady-state bleaching is proportional to the square root of the intensity of absorbed light and that it varies with an uncontrolled factor, the concentration and the chemical nature of an unknown impurity. *I* indicates the intensity of the absorbed light (in appropriate units) and k, is the rate constant for the i^{th} reaction step.

For some dyes, there is even degradation in a thermodynamic process. This was observed on acridine orange (AO) and acridine yellow (AY) by N. I. Surovtseva and his coworkers {{60 N. I. Surovtseva, N. P. Smirnova, A. M. Eremenko, T. V. Fesenko, and V. A. Pokrovsky 2010}}. It was concluded that the degradation process depended on the dye structure, stability, and tendency to aggregate on the semiconductor surface. Effective photodegradation of the acridine dyes occurred through the following stages: 1, demethylation (AO) or loss of an amino group (AY); 2, photodimerization; 3, photodegradation.

2.6 Effective parameters on quantum yield

In the photodynamic process there are a lot of possible parameters influencing the yield of singlet oxygen. The previous researchers did much work on parameters such as dye concentration, pH and temperature. In a German group, they made the conclusions on Rose Bengal research {{61 M. Scha¨ fer, C. Schmitz, R. Facius, G. Horneck, B. Milow, K.-H. Funken and J. Ortner 2000}}. By controlling the concentration and making comparisons with control group, they observed that the effective concentration was 1 ppm to 5 ppm. And in this range, the $^1O_2$ production rate under normal conditions (T=25^{o}C, pH=7.0) increased proportionally with increasing RB concentrations. At concentrations higher than 5 ppm, RB was toxic by itself. The influence of temperature was investigated in a range from 10 to 35^{o}C with 2 ppm RB and pH = 7.0. The results did not show a strong correlation of $^1O_2$ production rate and variation of temperature. Furthermore, $^1O_2$ production rate was the same for the variation of pH indexes.

Some organic dye photosensitizers have a high quantum yield and they can be grafted to fabric surface which requires bridge polymer. This is a new way to dye fabric and it makes the fabric look regular and work more functional.

2.7 Bridge polymer---poly (acrylic acid) (PAA)

Acrylic monomers are highly reactive chemicals and, therefore, are useful, nearly exclusively as intermediates in the production of other materials. Individual molecules of acrylic acid readily combine with themselves to form long chains of repeating units, or "polymers". The polymers have completely different physical and chemical properties than the constituent monomers. Scheme 2.6 shows poly (acrylic acid) (PAA) formula.

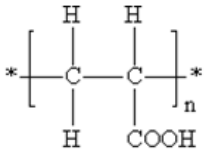

Scheme 2.6: Polyacrylic acid (PAA) formula

It is widely used in manufacture of hygienic products, detergents, and waste water treatment chemicals. Another important application which has often appeared in research is surface grafting. PAA has many carboxylic acid groups that can be easily attached to many polymers as a cross media or reactive part. In Siqiang Zhu and Douglas E. Hirt {{62 Siqiang Zhu, Douglas E. Hirt 2009}} found that acrylic acid (AA) monomers penetrated into the polypropylene (PP) fiber and polymerized inside. PP fiber dimension enlarged significantly upon grafting with PAA. Moreover, the dynamic contact angle results show that the advancing water contact angle on single fibers decreased from 100˚ to 55˚ by grafting of

PAA, which means the grafting of PAA improved the wettability of PP fiber a lot. This research is strong evidence that PAA can be a very effective bridge after it is grafted on other materials. It is reported in US 2009/0317434 A1 {{63 He-Hsing Wu, Nini-Chen Tsai,Lie-Hang Shen, Bin Lin, Chia-Chieh Chen, Wuu-Jyh Lin 2009}}patent that grafting PAA on nylon or PET fibers is a useful intermediate to assist silver particles in adhering firmly onto nylon or PET fiber surface so that they can easily react with enzyme-protein molecules in bacteria and achieve sterilization effect by destroying the cell surface and killing the bacteria. PAA grafting layer was also found to affect the diffusion and solubility coefficients of different gases through the surface-grafted films {{64 Vanina Costamagna, Miriamstrumia, Marlo'Pez-Gonza'Lez, Evaristo Riande 2006}}. In this study, the transport of oxygen, nitrogen, carbon dioxide, argon, carbon monoxide, methane, ethane, ethylene, and propane through PAA grafted polyethylene film is investigated and about 80% reduction in permeation of the film was observed.

2.8 Effect of some factors on grafting yield

The grafting process depends on many factors such as temperature, reaction time, pressure and acrylic acid (AA) concentration. There are many similar studies in this field. In Hou's study {{65 Zhenzhong Hou, Qun Xu, Qi Peng, Jianbo Li, Haijuan Fan, Shijun Zheng 2006}}, the reaction time varied from 2 hours to 12 hours. It was observed that the grafting efficiency increased from 40.5% (2 hours group) to 56% (12 hours group). And from a trend analysis, it was concluded that the grafting efficiency could be enhanced continuously with time. This effect was analyzed elsewhere {{66 Guoqi Fu , Haiyan Li, Haofeng Yu, Li Liu, Zhi Yuan,

Binglin He 2006}} and similar conclusions were made by the authors. In the same study, Hou found the grafting efficiency was enhanced with increasing reaction pressure. By trying different experiments, he determined that the best temperature for PAA grafting was 55℃. He described the relationship of temperature and grafting efficiency like this: grafting efficiency initially increased with increasing temperature and reached maximums at 55℃. When the temperature reached 60℃, the polymerization system is completely impregnated, so no more increase would be achieved. We can find a similar result in another study {{66 Guoqi Fu , Haiyan Li, Haofeng Yu, Li Liu, Zhi Yuan, Binglin He 2006}}. For the same reason, acrylic acid concentration has the same effect with temperature on grafting efficiency.

2.9 Grafting onto nylon

In recent years the scientific literature has revealed a growing interest in graft copolymerization on textiles as a method for allowing modification of the properties of textile fabrics without changing the manufacturing process. Many articles concerning this process have concentrated on the addition of carboxylic groups into fibers either to improve their hydrophilic properties or to prepare the fibers for further modification, resulting in new properties such as antistatic and antibacterial characteristics or heat resistance. Graft copolymerization of vinyl monomers onto polyamide was found to be an important modification because it improves the following properties: moisture sorption and swelling, dye-ability, and thermal stability as well as reduction of moisture sorption. More and more studies of grafting on nylon fiber, yarn or fabrics are being done these years. The

polymerization reaction of acrylonitrile (AN) grafting onto nylon-6 fabric was described as the following equations {{67 S. H. Samaha, D. M. Essa, F. M. Tera 2004}}:

$$AN + R^{\bullet} \rightarrow RH + AN^{\bullet}$$
$$AN^{\bullet} + n_1 AN \rightarrow PAN$$
$$\text{Nylon-NH} + R^{\bullet} \rightarrow RH + \text{Nylon-N}^{\bullet}$$
$$\text{Nylon-N}^{\bullet} + AN \rightarrow \text{Nylon-N-AN}^{\bullet} \xrightarrow{+n_2 AN} \text{Nylon-grafted-PAN}$$

where $R^{\bullet}$ is a free radical species, $AN^{\bullet}$ is activated AN molecules, PAN is polyacrylonitrile homopolymer, $\text{Nylon-N}^{\bullet}$ is nylon macroradical. With this mechanism, it is reported that acrylonitrile monomer was successfully grafted into nylon fabric. The IR analysis showed a new band for the grafted nylon, making sure of the presence of grafted chains of polyacrylonitrile in nylon backbone structure. The thickness of nylon fabric was increased from 1.555mm for the ungrafted one up to 1.931mm for the grafted fabric with a graft yield of 58.4%. In another paper {{68 Finn Andrew Tobiesen, Stephen Michielsen 2002}}, the researchers found that PAA was grafted via an amide linkage to the naturally occurring amine ends of nylon 6,6 using 1-ethyl-3-(3 dimethylaminopropyl) carbodiimide hydrochloride (EDC)-activated amidization. XPS was used to characterize the grafting efficiency in this study. A large fraction of the surface was found to be consistently converted to PAA via grafting using a PAA 250 K polymer at room temperature in 30 min using a large excess of EDC. The same amount of grafting was verified to be possible with less EDC at higher temperatures. This research also pointed that the most interesting feature of covalently attaching PAA to the surface is that PAA can then act as a scaffold to attach other molecules

to the surface that can further improve the physical and chemical properties of the surface of the film. This method can be used to increase (or decrease) the hydrophiliciy of the nylon surface. Jadwiga Buchenska {{69 Jadwiga Buchen Ska 2001}} did some research on grafting poly-(acrylic acid) onto nylon yarn. He concluded that an effective process for the grafting of poly-(acrylic acid) on polyamide yarn has been developed by using the addition of a dispersing agent and an activator in the grafting bath. And with the calculation factors such as the reaction efficiency, the extent of reaction and the ratio of grafting, the conditions of grafting have been found under which the by-product (homopolymer) can be reduced or eliminated, which provides a highly economical grafting process for fiber modification.

2.10 Photostability of nylon

A considerable disadvantage of polyamide fibers is their low light resistance. This leads to changes in their appearance and their physicomechanical parameters under ambient atmosphere conditions and as a result of the effect of sunlight. Fabric made of polyamide fibers may face a lot of problems when it is for outdoor applications because they may fade or degrade due to photodegradation or oxidation of dyes on the surface.

2.11 Photodegradation of nylon 66 and nylon 6

Polymeric materials have shown significant morphological changes in polymers when they are exposed to shorter wavelength uv or high energy irradiation (x-ray, gamma, electrron). Generally, high energy irradiation destroys crystallinity and usually forms crosslinking in vacuum, but chain scission mainly occurs in air. Photodegradation of nylon 66 has been

studied principally with its photodecomposition and changes in tensile properties when they it is exposed out-of-doors or to broad-band irradiation sources in the laboratory. There is a report {{70 R. E. Forens, R. D. Gilbert, B. S. Stowe, G. P. Cheek 1973}} of photodegradation of nylon 66 based on the tensile data which shows the important mechanical properties of textiles.

In related literature {{71 B.S. Stowe, V.S. Salvin, R.E. Fornes R.D. Gilbert 1973}}, nylon 66 yarn was exposed to near-ultraviolet radiation in a dry oxygen atmosphere for exposure periods of 240 hr. The ultraviolet (UV) effects were assessed by viscosity and density measurements, acid dye take-up, wideline nuclear magnetic resonance (NMR), and differential scanning calorimetry (DSC). It was reported that nylon 66 yarn exposed to UV irradiation in the presence of dry-oxygen exhibited measurable changes in fine structure. Anionic dyeing was found sensitive to small changes in fiber structure and hence detected UV effects at low exposure times. It revealed constriction of the fiber structure, but not the nature of the constriction. Wideline NMR detected significant change in fiber morphology only after 240-hr uv exposure. The study also indicated that photo-oxidation at a low energy level causes considerable chain scission and reduction in molecular weight as revealed by intrinsic viscosity and reduction in second moment measured at high temperatures. Wideline NMR and DSC measurements suggested electromagnetic radiation of 350 nm does not cause major disruption of crystallites and permanent scission must have occurred primarily in amorphous regions of the fiber. It was concluded that under the experimental conditions of

this study, no measurable crosslinking occurred because no insoluble gel was detected in 90% formic acid, nor did wideline NMR indicate crosslinking.

The photodegradation of unprotected bright nylon-6 fiber by exposure to daylight and in the fadeometer has been studied by previous researchers {{72 R.V.R. Subramanian, T.V. Talele 1972}}.The degradation was found to be caused by a random scissionof the C-N bonds of the polymer chain because there was an big fall in the tensile strength and viscosity average molecular weight of the polymer. But the polymer chain was not affected appreciably so as to cause any changes in its infrared spectrum. It was concluded that the there were two stages in photodegradative breakdown of nylon 6 fiber. In the initial stage of exposure, peroxides formed and the nonvolatile watersoluble degradation products were found formed in the prolonged exposure.

2.12 Factors affecting photodagradation of nylon

2.12.1 Sulfur dioxide in air

From Zeronian's study {{73 S.H. Zeronian, K.W. Alger, S.T. Omaye 1973}}, the degradation of nylon 66 fabric by exposure to light and air is increased if the air is contaminated with sulfur dioxide. By comparing the chemical properties of fabrics exposed to light and air with those of fabrics exposed to light and air containing 0.2 ppm sulfur dioxide, he found evident additional degradation from the sulfur dioxide containing group. The increased degradation was also indicated by the differences in tensile properties of yarn taken from fabrics. The chemical properties and yarn tensile properties of nylon fabric

hydrolyzed with sulfuric acid or hydrochloric acid and of nylon fabric irradiated with light in the presence of sufuric acid also were measured to provide comparisons with the degradation of nylon by exposure to sulfur dioxide. The effect of degradation by light and air contaminated with sulfur dioxide was significant.

2.12.2 UV absorber

Since the photodegradation of nylon-6 fiber is caused mainly by ultraviolet light, attempts have been made to improve the resistance to such degradation by applying UV absorbers {{72 R.V.R. Subramanian, T.V. Talele 1972}}. It was assumed the presence of such UV absorber on the surface of the fiber could result in the absorption of incident UV light, thus reducing the degree of degradation to a certain extent. Therefore a UV absorber, viz 2,2'-dihydroxy, 4,4'-dimethoxy benzophenone, was applied to the fabric and has been found to be effective in reducing the extent of photodegradation. However the efficiency of UV absorber is restricted by the normal scouring of fabric. In order to determine the efficiency of such UV absorbers after scouring, the UV absorber-treated fabrics were scoured twice, conditioned under standard atmospheric conditions and then tested for different characteristics. The results showed that there is some reduction in the efficiency of UV absorber after scouring.

Other factors such as relative humidity, dye stuffs, dyeing auxiliaries, and anti-oxidants were all indicated to be effective parameters in degradation of nylon.

2.13 Dyeing of nylon

The presence of terminal amino end groups in nylon fibers imparts substantivity towards anionic dyes, specifically acid dyes, direct dyes and reactive dyes. So the colouration of nylon is usually achieved with acid dyes. These attach to the nylon via ion-ion linkages between the cationic, protonated, amino end groups of the nylon (NH_3^+) and the anionic sulfonate residue of the dye (Dye-SO_3^-). Generally, the dyeing process is a solid/liquid phase process, which proceeds by the movement of the dye molecule from the liquid phase to the solid surface of the fiber by virtue of its affinity, and then diffusion takes place inside the fiber. Therefore, the first process would be a fast adsorption controlled process and, afterwards the dye molecules getting into the fiber starts to take place by the second slow process, which is diffusion controlled. The conventional acid dyeing of nylon 6 fiber was depicted as {{74 Huei-Hsiung Wang, Chyung-Chyung Wang 2005}}:

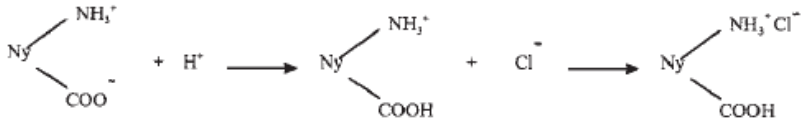

and then

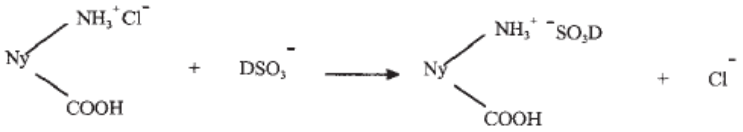

Scheme 2.7: Dyeing process of nylon

where Ny means nylon, D refers dye. As can be seen in Scheme 2.7, nylon first absorbs a proton combined with a chlorine ion on the fiber. Finally the chlorine ion is replaced by a sulfuric anion of acid dye because of the high affinity of the dye acid anion. In all, in the conventional dyeing method, an acid dye forms an ionic bond of a D-SO_3Na structure in the dye bath.

2.14 Factors influencing dyeing of nylon

2.14.1 Ultrasound pretreatment

Considering the general dyeing process, something can be used to speed up the second process so as to increase the dyeing rate. From the previous research by MM Kamel {{75 MM Kamel, Reda M El-Shishtawy, HL Hanna, Nahed SE Ahmed 2003}}, it was determined that the use of power ultrasonics (38.5kHz, 350W) can improve the dyeability of nylon-6 fabrics with reactive dyes. The results of factors affecting dyeability have indicated that ultrasound was an effective technique in increasing the color-strength values of dyed fabrics in comparison with those without ultrasound. It was pointed that ultrasonic power influences the rate of dyeing mainly by de-aggregating the dye molecules and increasing the diffusion rate inside the fiber. In his following study {{75 MM Kamel, Reda M El-Shishtawy, HL Hanna, Nahed SE Ahmed 2003}}, the effect of ultrasound on fiber fine structure and its effect on the dyeing rate with different reactive dyes were investigated. By detecting the kinetic data for nylon 6 fiber with different reactive dyes, he concluded that ultrasound pretreated fiber showed better rate enhancement of dyeing especially in the stage of dye

diffusion inside the fiber. Moreover, applying ultrasonic in accelerating the dyeing rate proves suitable for those systems of dyeing, which hardly achieve good dyeability by conventional methods. At the same time X-ray diffraction analysis proved that ultrasonic waves simultaneously affect the fine structure of nylon 6 fiber during the dyeing process by increasing the percentage of its crystallinity.

2.14.2 Dyeing pH

pH value is a very important parameter for dyeing process. For nylon dyeing with reactive dyes, previous related study {{76 A. Soleimani-Gorgani1, J.A. Taylor 2008}} pointed out: At high pH the build up and fixation of anionic reactive dyes on nylon is limited by electrostatic repulsion between dye and anionic carboxylate groups present in the nylon. At low pH the effective concentration of anionic carboxylate groups is greatly reduced, and that of cationic protonated amino groups increased, leading to electrostatic attraction between dye and fiber but a massive reduction in the concentration of free amino groups. In another similar study {{77 S.M. Burkinshaw, K. Lagonika, D.J. Marfell 2003}}, maximum color strength was achieved at pH 7.

2.14.3 Dyeing temperature

In the same study {{77 S.M. Burkinshaw, K. Lagonika, D.J. Marfell 2003}}, the effect of dyeing temperature was discussed. Five dyes varied in terms of the effect of dyeing temperature on color strength in this research. For two of the dyes, color strength increased markedly with increasing application temperature and reached a maximum at 98 to 110°C

whereas the depth of shade achieved for the remaining three dyes only very gradually increased with increasing temperature from 50 to 120 °C. Generally, the author thought temperature had little effect on color of the dyeing within the range 70 to 98 °C whilst both lower temperatures (50 and 60 °C) and, especially, higher temperatures (110 and 120 °C) imparted marked color change. Dyeing temperature was verified to have little effect on the fastness to light of dyeing and repeated washing.

Use of photoactive dyes allows the production of singlet oxygen. These dyes can be attached to the surface of fibers using PAA as a modifier. In the next chapter, the experimental protocols are described for attaching Azure A to nylon via PAA and a series of test methods on different properties of experimental samples. In Chapter 4, the results of these experiments are presented and discussed.

3. Experimental Methods and Procedures

3.1 Approach of This Research

The approach of this research was to determine the photostability of two dyes, Azure A and Rose Bengal, when they are in aqueous solution, when they are physically adsorbed onto glass filter paper, and when they are chemically bonded to the surface of a nylon nonwoven. A comparison is made between different dyes from their performance when they were exposed to light from a tungsten lamp. Rose Bengal and Azure A were selected based on their chemical structure. Both of these chemicals are water soluble and can be easily attached to polymers. They both have a high singlet oxygen quantum yield so they can be used as photo-sensitizers. The aim was to explain the photostability from different aspects and get a better product for potential customers.

3.2 Experimental Materials

3.2.1 Rose Bengal

Rose Bengal was selected because it holds an important position among all dyes for a number of reasons. The most important is that it is a water soluble photodynamic sensitizer, and it has a large absorption in all solvents in which it is soluble. Furthermore, its triplet state is completely quenched by molecular oxygen which leads to a high singlet oxygen quantum yield while its singlet state may be quenched by strong oxidizing agents {{78 D. C. Neckers 1989}}. It was donated by LAAMScience. The chemical structure is shown in Figure 3.1.

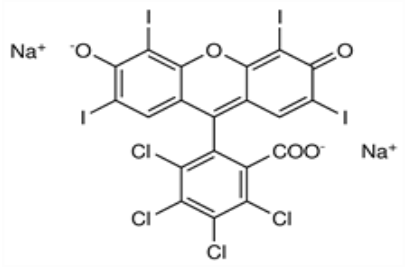

Figure 3.1: Chemical structure of Rose Bengal

3.2.2 Azure A

Azure A was purchased from Sigma-Aldrich (St. Louis, MO). It was selected because of its color which is liked by most customers. Azure A also has a high singlet oxygen quantum yield. The chemical structure of Azure A is shown in Figure 3.2.

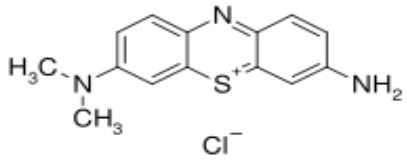

Figure 3.2: Chemical structure of Azure A

3.2.3 Furfuryl Alcohol (FFA)

Furfuryl alcohol (FFA) which was purchased from ScienceLab (Houston, NJ) is used in the singlet oxygen generation test. If FFA's color turns yellow or brown, it should be distilled before use in this study. The photo-oxidation of FFA in water sensitized by naturally occurring dissolved organic materials under visible light has been shown to proceed almost exclusively by a singlet oxygen mechanism. FFA does not physically quench singlet

oxygen. It was thus recommended as a highly soluble, efficient trapping agent for singlet oxygen determinations in natural waters {{79 Werner R. Haag, JUrg Hoigne, Ernst Gassman, Andre M. Braun 1984}}.

3.2.4 Poly-(acrylic acid) (PAA)

Poly-(acrylic acid) which was purchased from Sigma-Aldrich (St. Louis, MO) is widely applied in the grafting of polymers according to the previous literature. In this research, PAA was grafted onto nylon fabric in the preparation work of dyeing nylon. It acts as a mediator between dye and fabric. In later finishes, dye was attached to the fabric through PAA which was previously grafted on the fabric.

3.2.5 4-(4,6-dimethoxy-1,3,5-triazin-2-yl)-4-methylmorpholinium chloride (DMTMM)

DMTMM purchased from Sigma-Aldrich (St. Louis, MO) is used as a condensing reagent in the dyeing process to promote bonding of PAA to nylon.

3.2.6 Fabric Used

Cerex Spectramax® (Cantonment, FL) white nylon 6, 6 spunbond fabric with basic weight 35gsm, was provided by LAAM Science (Morrisville, NC).

Modified nylon 6, 6 spunbond fabric was also provided by LAAMScience. Rose Bengal was attached to the surface of this fabric.

3.3 Experimental Procedures

3.3.1 Finishing Process

A 5% PAA (by weight) solution in water was made at room temperature. After all PAA was dissolved, 1mole % Azure A relative to the amount of PAA repeat units was added to the PAA solution. After 1 hour stirring, the same number of moles of DMTMM as Azure A was added to the mixture. After another 3 hours stirring, 0.3 grams DMTMM was added into the mixture again. Then the dye solution was left stirring for more than 1 hour. After the Azure A-g-PAA solution was prepared, a piece of the Spectramax® fabric was immersed into the dye solution. Then the immersed fabric was padded by a pad machine (Figure 3.3) with a wet pick up of 100%. The padded fabric was finally put into the oven (Figure 3.4) for 1 minute at a temperature of 170 ℃.

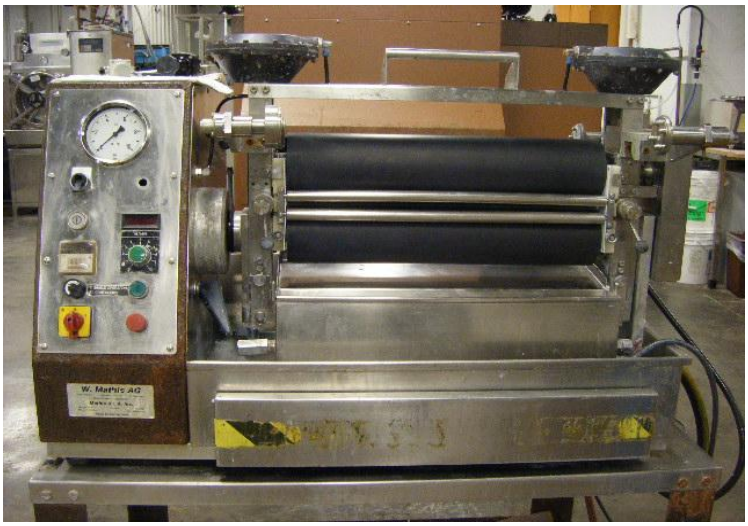

Figure 3.3: W. Mathis AG HVF 24489 pad

Figure 3.4: Werner Mathis AG LTF 134489 hot air oven

3.3.2 Properties of Dye in Solutions Testing

3.3.2.1 Ultraviolet-Visible Spectrophotometry (UV/Vis) Testing

3.3.2.1 Adsorbed Dyes on Glass Filters

3.3.2.1.1 Sample Preparation

Aqueous solutions of Rose Bengal and Azure A solutions were made at concentration of 20 μM. Then Type A/E Glass Fiber Filter paper (50mm), which was purchased from PALL Life Sciences was immersed into the solutions. Next they were placed in Fisherbrand® petri dishes (15mm) separately. The water was allowed to evaporate in a dark space where there should be as little light as possible. Then the petri dishes were placed under a 200 watt incandescent bulb. The light intensity, which was between 13500 Lux and 16500 Lux, was measured by a Mestech brand digital light meter (Model: LX 1330B).

3.3.2.1.2 Light Exposure Process

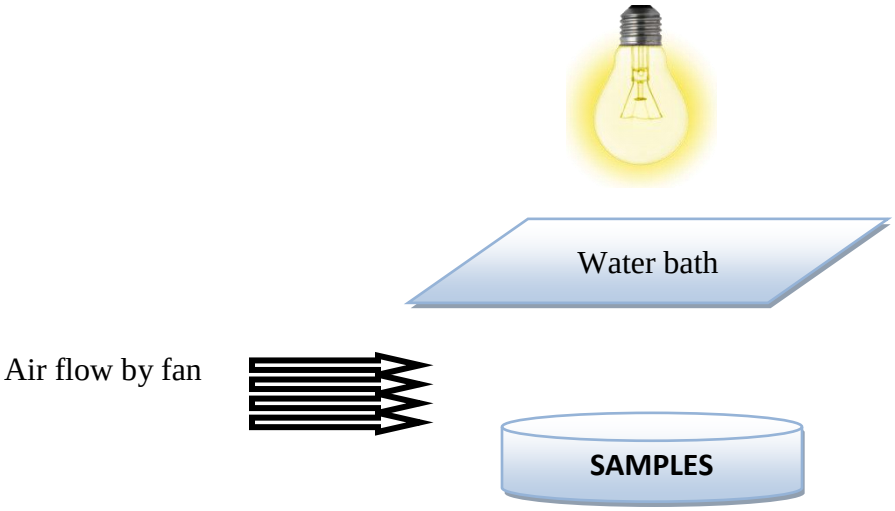

Figure 3.5: The UV test treatment diagram

There were 5 groups for Rose Bengal and 6 groups for Azure A. The control groups were not exposed to light. The remaining groups were exposed to light for 1, 2, 4, 8 and 16 hours separately. A water bath and a small fan were used in the system to avoid heating caused by infrared light from the lamp. The experimental setup is shown in Figure 3.5.

Figure 3.6: Thermo Scientific Genesys 10 UV-Vis scanning machine

[Source: http://www.berca-indonesia.com/pub/thermo_uvisible.htm]

After exposure the dyes were redissolved with water (5ml). Then the solutions were placed into the Thermo Scientific Genesys 10 UV-Vis scanning spectrometer (Figure 3.6) and the absorbance was measured.

3.3.2.2 Aqueous Solution Singlet Oxygen Generation Test

The singlet oxygen generation test followed Haag's procedure {{79 Werner R. Haag, JUrg Hoigne, Ernst Gassman, Andre M. Braun 1984}}. The same solutions as in the UV/Vis test were used in this test. The solution circulated in a system which is shown below in Figure 3.7. This is an open system and air was blown through the solution container. The solution went into a clear round chamber which was exposed to light and then went back into the container. The exposure times were 0, 1, 2, 4 and 8 hours for the experimental groups.

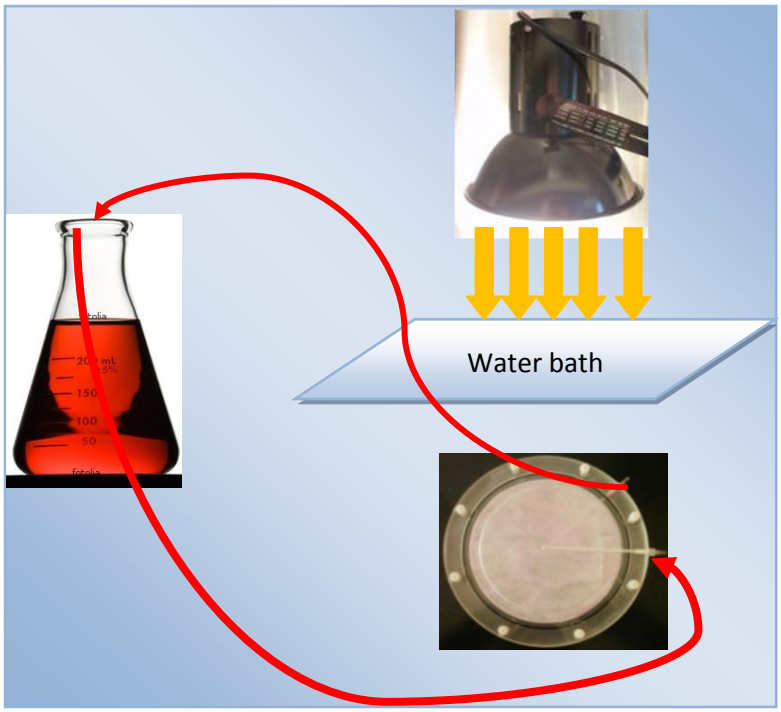

Figure 3.7: Light exposing treatment process

After exposure, the solutions were removed and mixed with FFA (100mM). The solutions were then placed back the system (Figure 3.8), which was then sealed to prevent additional oxygen from entering the system.

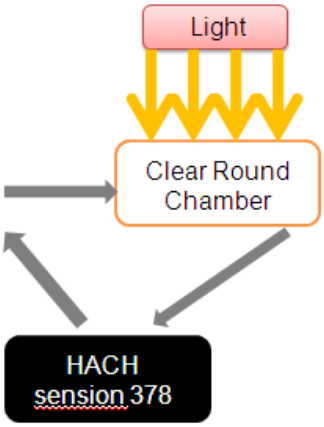

Figure 3.8: Sealed testing system

Figure 3.9: HACH Sension 378

The solution in the sealed system was circulated between the chamber and a Hach Sension 378 while the light was shining on the clear chamber. Hach Sension 378 measured the oxygen concentration data at 10 seconds intervals.

FFA traps the singlet oxygen produced in this sealed test system, so the oxygen concentration detected by Hach Sension 378 decreases because it is the only source of singlet oxygen. In this indirect way, we can get the efficiency of singlet oxygen generation.

3.3.3 Chemical Structure Detecting--Fourier Transform Infrared Spectroscopy (FTIR) Test

Saturated Rose Bengal and Azure A solutions were made in petri dishes. The petri dishes

were dried in a dark place until films formed in the petri dishes. Then the petri dishes were cut into $1\times1cm^2$samples. The same light source was used to treat these samples for different time periods at 20,000 lux light intensity. A Perkin-Elmer Spectrum 100 FT-IR Spectrometer (Figure3.10) was used to analyze those treated samples.

Figure 3.10: Perkin-Elmer Spectrum 100 FT-IR Spectrometer

3.3.4 Tests of dye bound to LaamScience Fabric

3.3.4.1 Color CIELAB 76 Test

3.3.4.1.1 Sample preparation

Fabric provided by LAAMScience and the finished fabric were cut into $30\times30cm^2$ pieces. These fabric samples were then treated with the same light source as above. The intensity was 20,000 lux and the exposure time of 0, 1, 2, 4, 8 and 16 hours were used.

3.3.4.1.2 Test

Hunter ColorFlex 45/0 was used to detect the fabric color intensity. The following parameters were selected: Scale: CIELab; Illuminant: D65; Observer: 10°; Procedure: None; MI Illuminant: Fcw; Display Mode: Absolute. The port size was 30 mm and there was no UV filter.

Before the sample testing, standardization was done using the standard surface (the same fabric without dyeing finish). Each sample was folded into 8 layers because usually more than 200 gsm sample is required for accurate readings. Each specimen was read 4 times for every observation. 4 different spots of the sample were chosen for average calculation.

3.3.4.2 Singlet Oxygen Generation Test

Instead of dye solutions, photo-bleached fabrics were placed into the clear round chamber. The same testing system and light source as for the solution test were used. A 100 mM FFA aqueous solution was first saturated with oxygen by bubbling air through it. This solution was then introduced into the testing system. The Hach Sension 378 system was used to record the oxygen concentration versus time. The data was analyzed to obtain the relative rates of singlet oxygen generation and is presented in the results and discussion chapter.

4. Results and Discussions

In this chapter, data from every test is represented and analyzed. It includes two different systems: aqueous system and fabric based system. UV/Visible spectroscopy, singlet oxygen generations, FTIR and color tests were performed. Trend line analysis is used and some simple statistical models were used to analyze the data.

4.1 Ultraviolet-Visible Spectrophotometry (UV/Vis) Testing

UV/Visible spectroscopy is a common and useful method to detect color change. As shown by the Beer-Lambert Law ($A = \varepsilon c \ell$), the amount of dye is closely related to a dye's appearance---color. *A* is absorbance, ε is the absorptivity, c is concentration and ℓ is the path length. So by comparing the absorbance curves, we can analyze the residual amount of dye. UV/Vis tests of adsorbed dyes on glass filter were performed first and are analyzed here. Absorbance curves of these dye samples are shown in Figure 4.1.

In Figure 4.1, Rose Bengal and Azure A's absorbance peak wavelengths are around 550nm and 640 nm, respectively. As the light exposure time increased, Rose Bengal's absorbance decreased from 0.78 to 0.36 while Azure A decreased from 0.79 to 0.26. This reduction indicates that the amount of dye decreased during the exposure time.

There are several possible reasons why dye disappeared in this process. The dyes are unstable under light; they may degrade or react with another component. As photosensitizers in this research, Rose Bengal and Azure A react with oxygen and they both form photoproduct. As their photoreactions occur, dyes will be degraded after a certain period.

From the absorbance curves of 8 hours light exposed Rose Bengal and 16 hours light exposed Azure A, we can see that there is very limited amount of them remaining. We can also reach this conclusion from the color change of these samples. The error bars for both samples are very small.

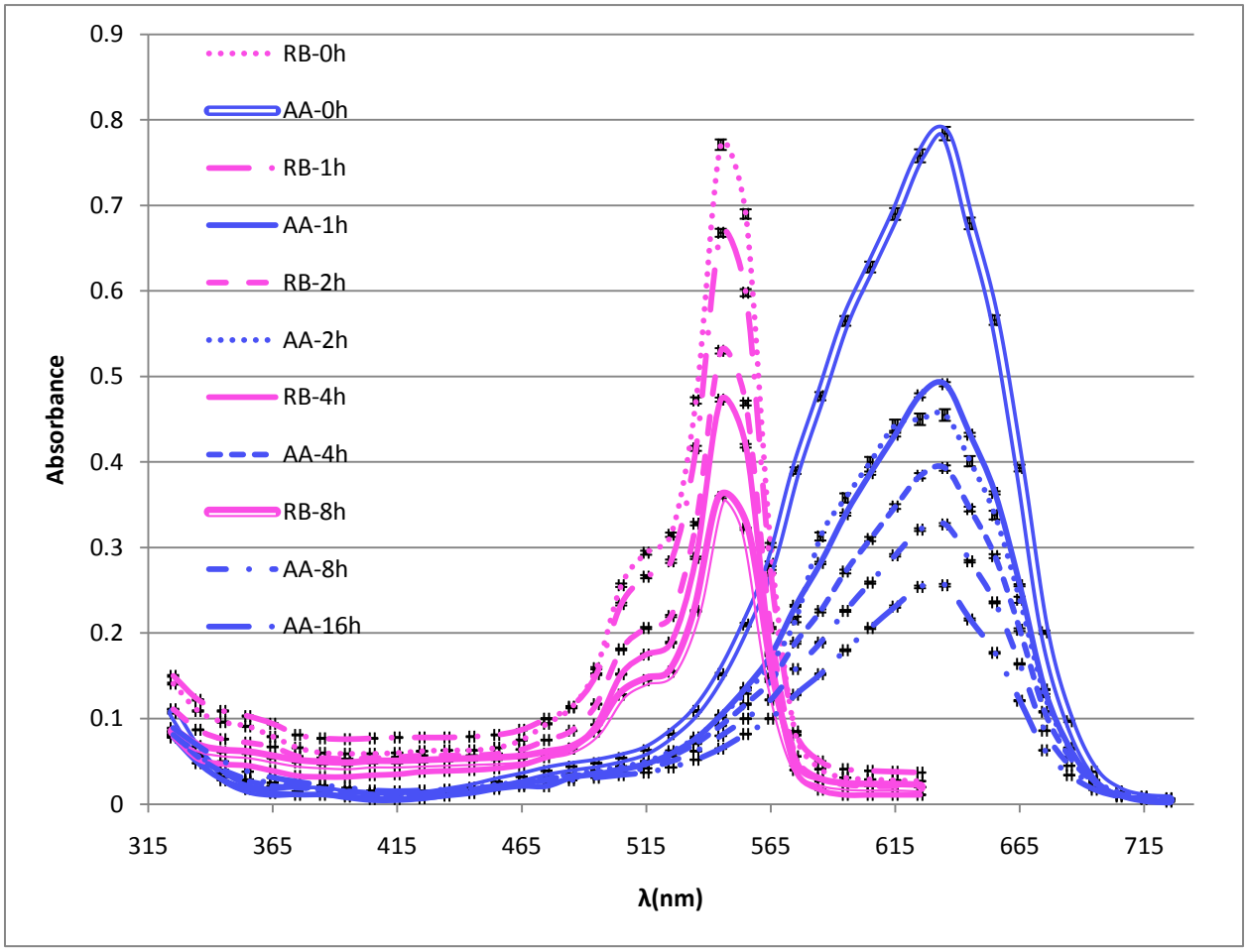

Figure 4.1: Rose Bengal (left) and Azure A (right) absorbance versus wavelength

The following picture (Figure 4.2) is Rose Bengal sample on glass filters. The color of these samples is lighter and lighter as exposure time increases. It is very difficult to get a

comparative group of Azure A samples because it fades very fast in the first hour but more slowly in the following couple hours.

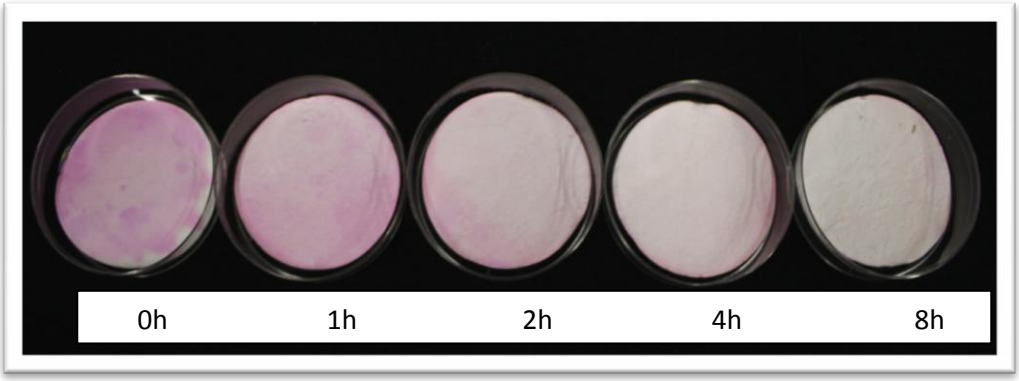

Figure 4.2: Rose Bengal on glass filter after exposed to light

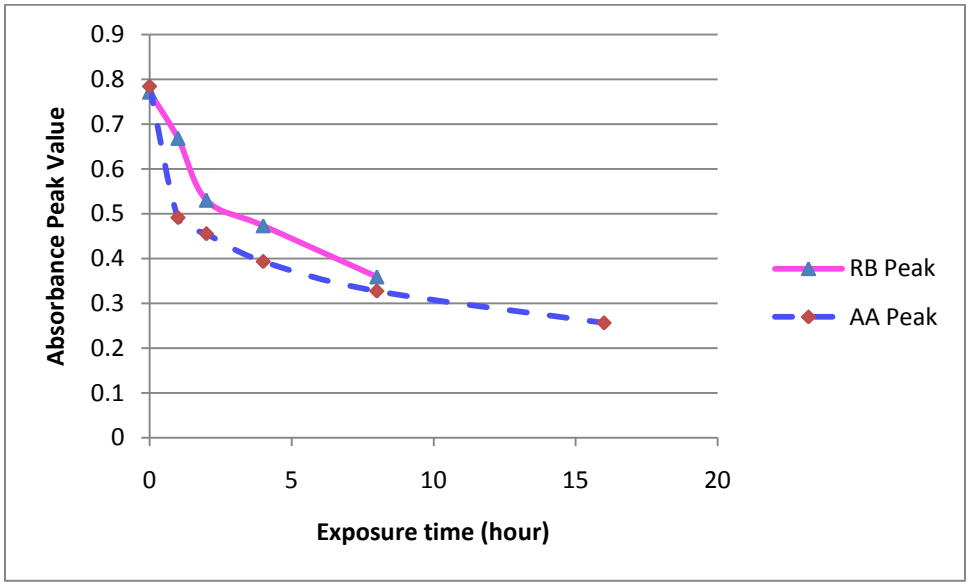

Figure 4.3: Rose Bengal and Azure A's absorbance peak value versus time result

Figure 4.3 shows Rose Bengal and Azure A's absorbance peak value versus time. Rose Bengal is stable in the first two hours, after that its absorbance began to fall very quickly. Azure A is different from Rose Bengal; it fell suddenly in the first hour and then decreased at

a slower rate. This phenomenon demonstrated that Rose Bengal is relatively more stable than Azure A. Azure A disappeared very fast at the beginning of this photoreaction. Rose Bengal performed well in the first period.

4.2 Aqueous Solution Singlet Oxygen Generation Test

The Rose Bengal solution singlet oxygen generation test result is shown below in Figure 4.4. It shows the oxygen concentration detected in the reaction system versus time. Kilo seconds is used as the times unit for better reading. A trend line analysis was done for every group. Every group was found to be well fit with exponential model $A = ae^{-kt}$.

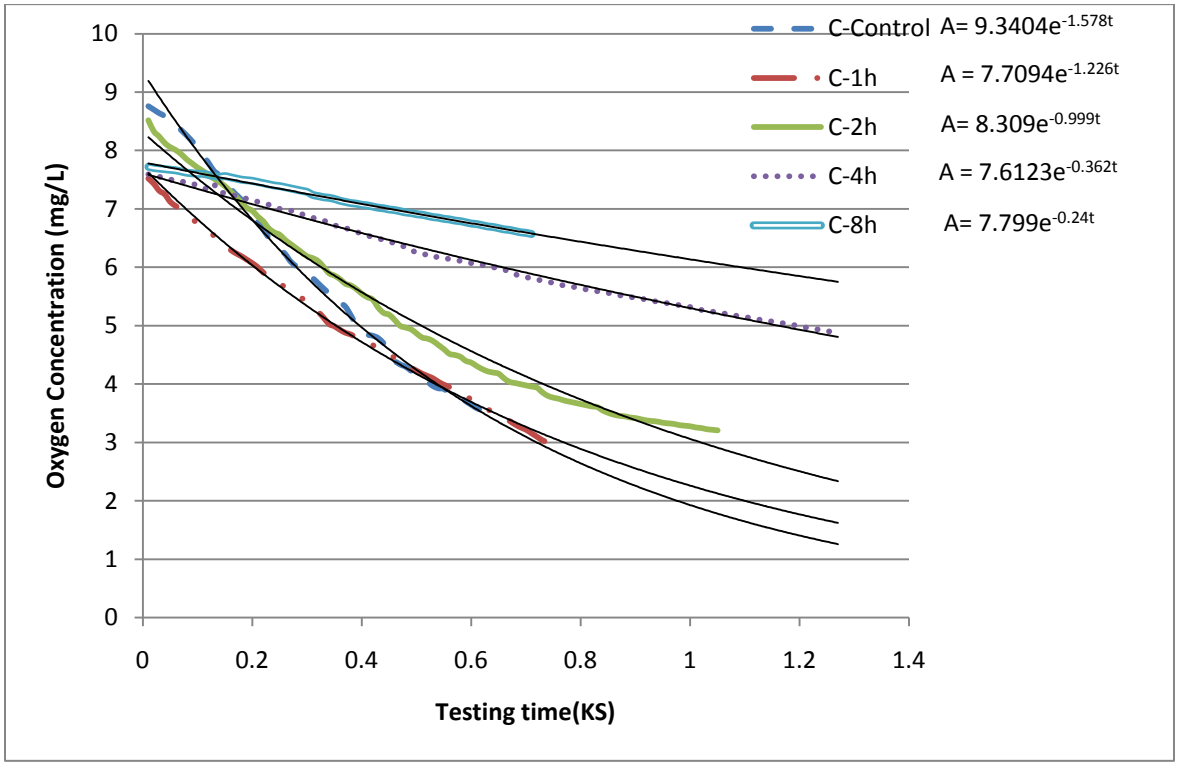

Figure 4.4: Rose Bengal solution singlet oxygen generation test result

The unit of the rate of decrease of the oxygen concentration, k, is ks^{-1}, which also indicates the photochemical reaction rate in this system. The equations in the upper right of the figure are the results for each group.

From the results in this figure, we found that k decreased from 1.58 to 0.24 ks^{-1}. The 8 hours light exposure group is much smaller than the control group (0 hour exposure to light). This result is consistent with the UV/Vis test too. The k values are graphed versus time in Figure 4.5(a); Figure 4.5(b) is the absorbance result from the previous test.

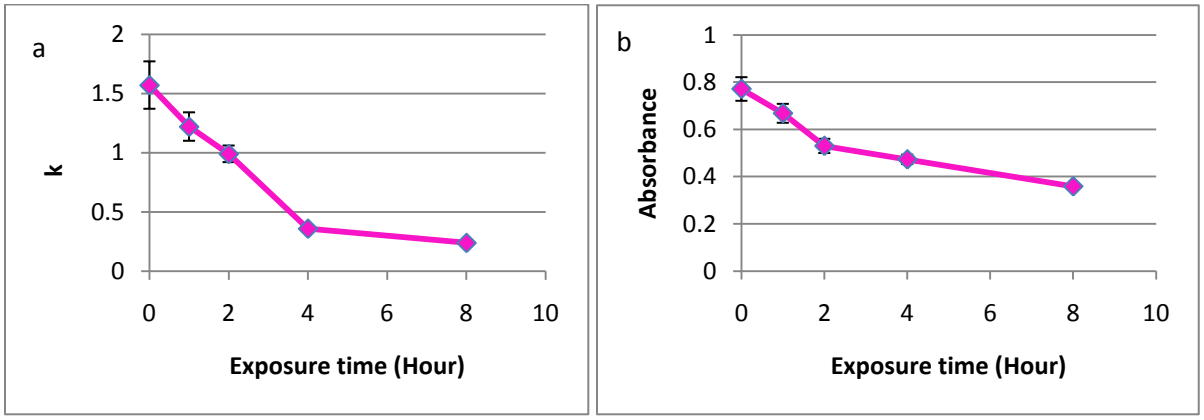

Figure 4.5: k versus time (a) and Absorbance versus time (b) for Rose Bengal

Figure 4.6 indicates the relationship between k and the absorbance. The data was fit using linear regression. The R value is 0.96 which indicates a very high dependence of k on absorbance.

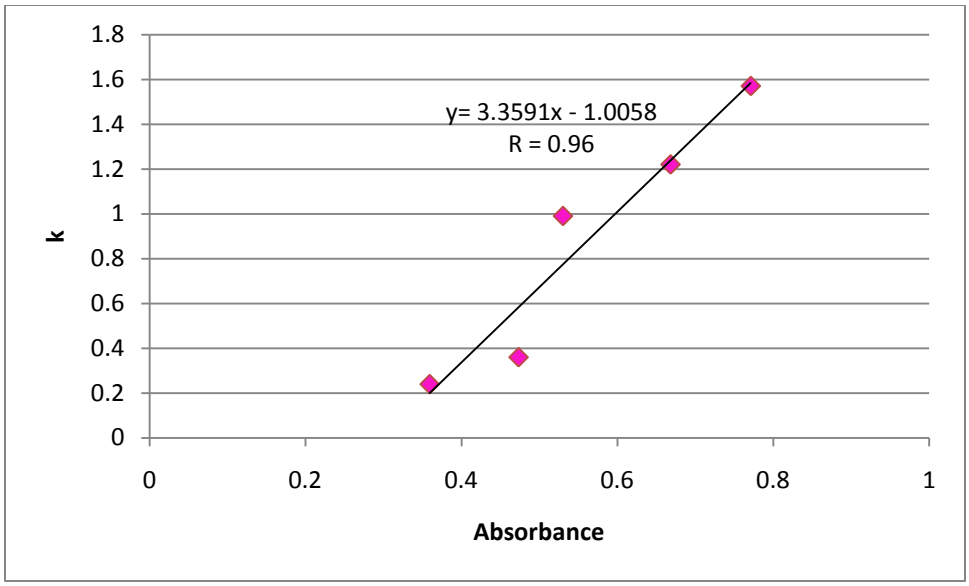

Figure 4.6: The relationship between k and absorbance for Rose Bengal

The linear model obtain from this line can be used in other related research. This will save a lot of time and energy because the UV/Vis test is easy and cheap. With this model we can use the absorbance data to derive k which directly demonstrates the photostability of the photosensitizers.

The same test was done on Azure A. Figure 4.7 is the Azure A test result. Every group fits the exponential model well. From the control group to the 1 hour treated group, the reaction speed decreased a lot which was indicated by the value of k ($0.602\sim0.265ks^{-1}$). The k value of 16 hours treated group is much smaller than the control group. For 16 hours group, $k=0.069ks^{-1}$. Thus almost no singlet oxygen was produced after 16 hours.

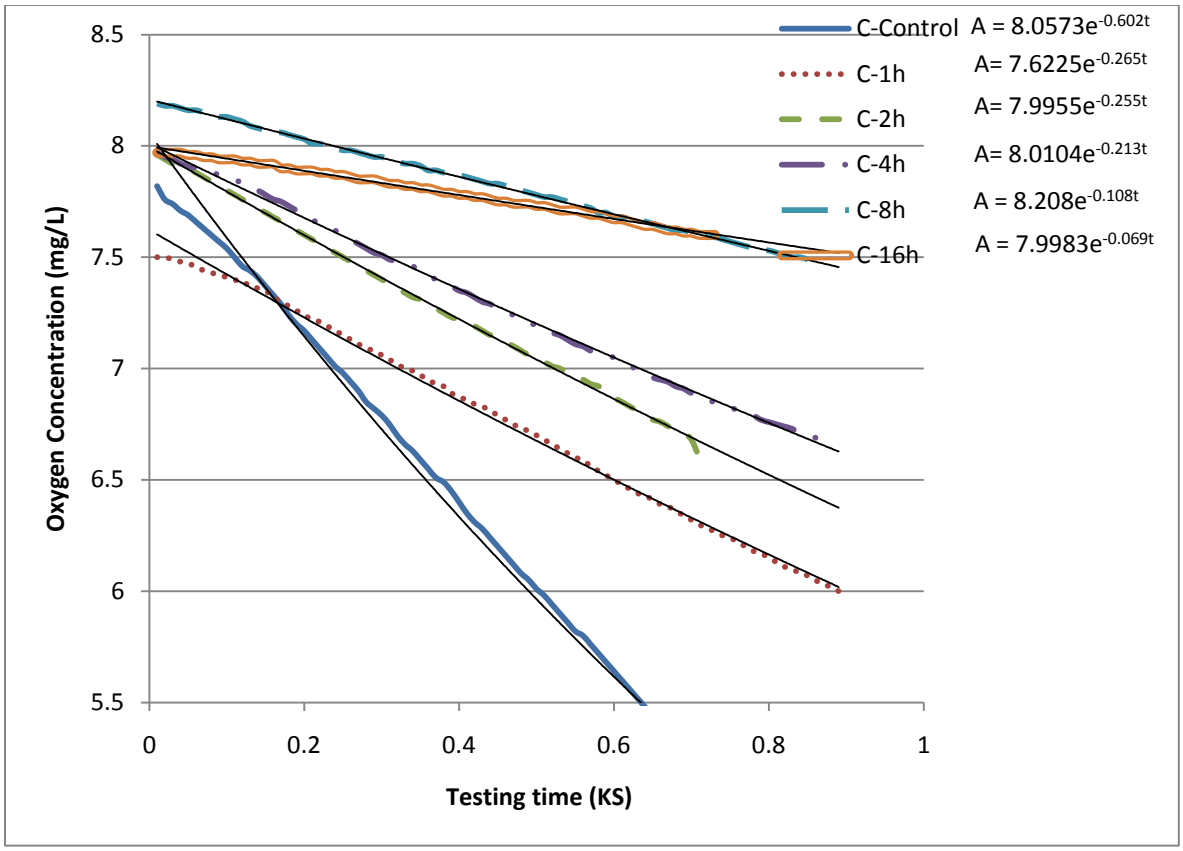

Figure 4.7: Azure A solution singlet oxygen generation test result

Figure 4.8 also shows the dependence of k on exposure time (a) and of the absorbance on time (b). These two curves seem very similar to each other.

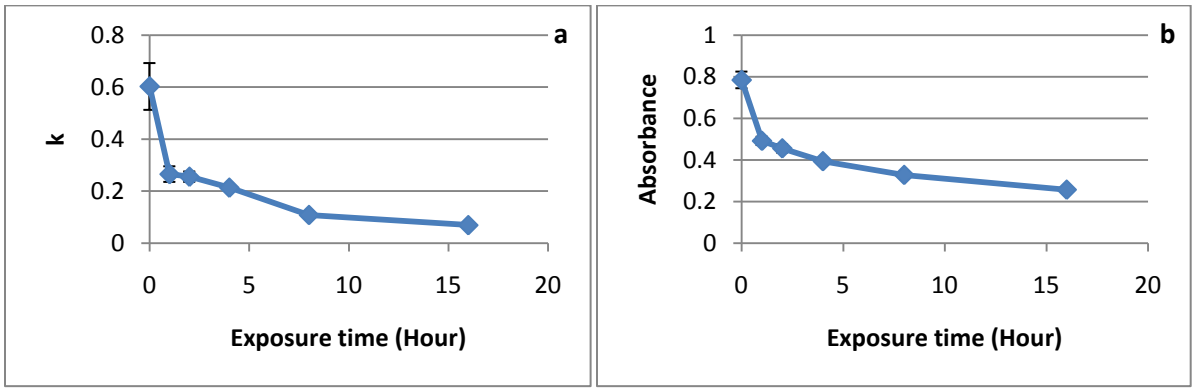

Figure 4.8: Relationship of time to k and absorbance for Azure A

The following Figure 4.9 shows the relationship of k to absorbance. Like the analysis to Rose Bengal, the R value and linear model were also obtained. R=0.99 indicates a very strong relationship between these two parameters.

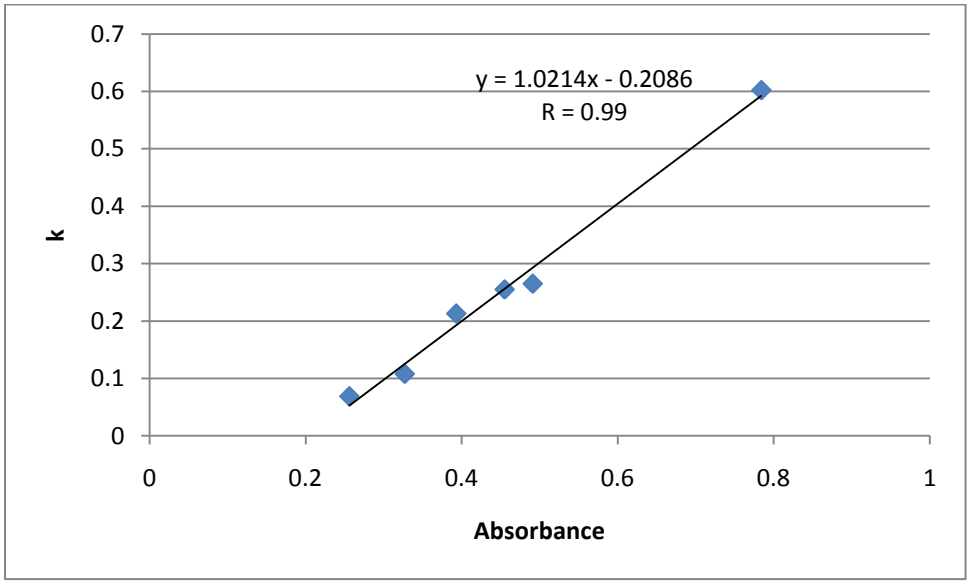

Figure 4.9: The relationship between k and absorbance for Azure A

4.3 Fourier Transform Infrared Spectroscopy (FTIR) Test

In an attempt to determine what chemical changes occur during photo-exposure, FTIR was measured on the dyes after light exposure. FTIR is known as a technique which is used to obtain an infrared spectrum of absorption of a solid, liquid or gas. An FTIR spectrometer simultaneously collects spectral data in a wide spectral range. This confers a significant advantage over a dispersive spectrometer which measures intensity over a narrow range of wavelengths at a time. FTIR technique has made dispersive infrared spectrometers all but obsolete (except sometimes in the near infrared) and opened up new applications of infrared

spectroscopy. FTIR is used in this research to detect the change of the chemical structure of Rose Bengal and Azure A through the difference of the spectra. Figure 4.10 is the Rose Bengal FTIR analysis result. The 3 spectra are from 0 hour group, 4 hours group and 8 hours group separately. The first peak around 3400 cm^{-1} is different for these three samples because the thickness of the samples is different, which is not related to the chemical structure change. However, there is an apparent change around 1400 cm^{-1}.

According to N. B. Colthup's research {{80 N.B. Colthup 1950}}, this might indicate the change of the bond between iodine and benzene ring or the carbon chlorine bond because they are the easiest to break. They may be oxidized by oxygen in the reaction process.

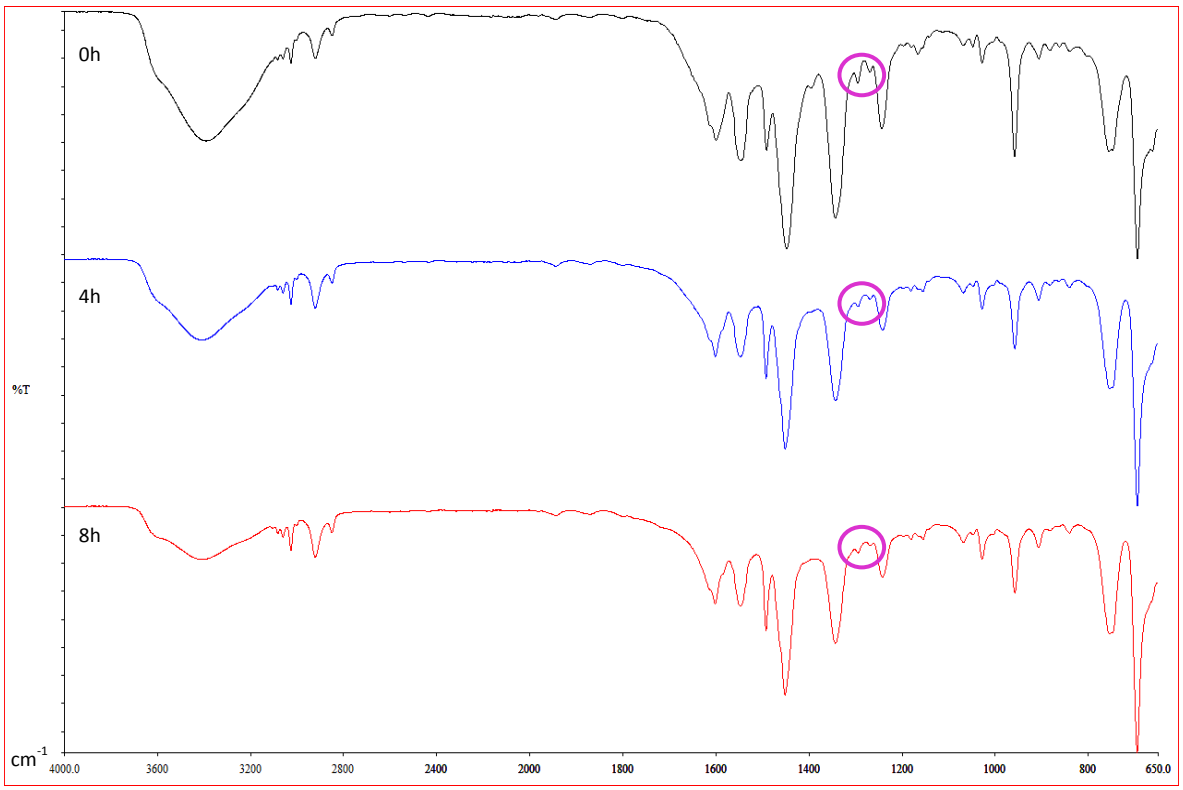

Figure 4.10: Rose Bengal FTIR result

Azure A's result is shown in Firgure 4.11. Similarly, the change of Azure A also appears in the finger print region. As marked on the curves, around 1450 wave number and 1350 wave number there are differences. 4 hours group and 8 hours group show similar result which is consistent with the previous result: Azure A changed a lot in the first step of reaction but only changed slowly in the following steps. The difference between the control group and 4 and 8 hour groups suggests the NH_2 group change {{80 N.B. Colthup 1950}}. The carbon nitrogen bonds in this group were broken in the photoreaction process.

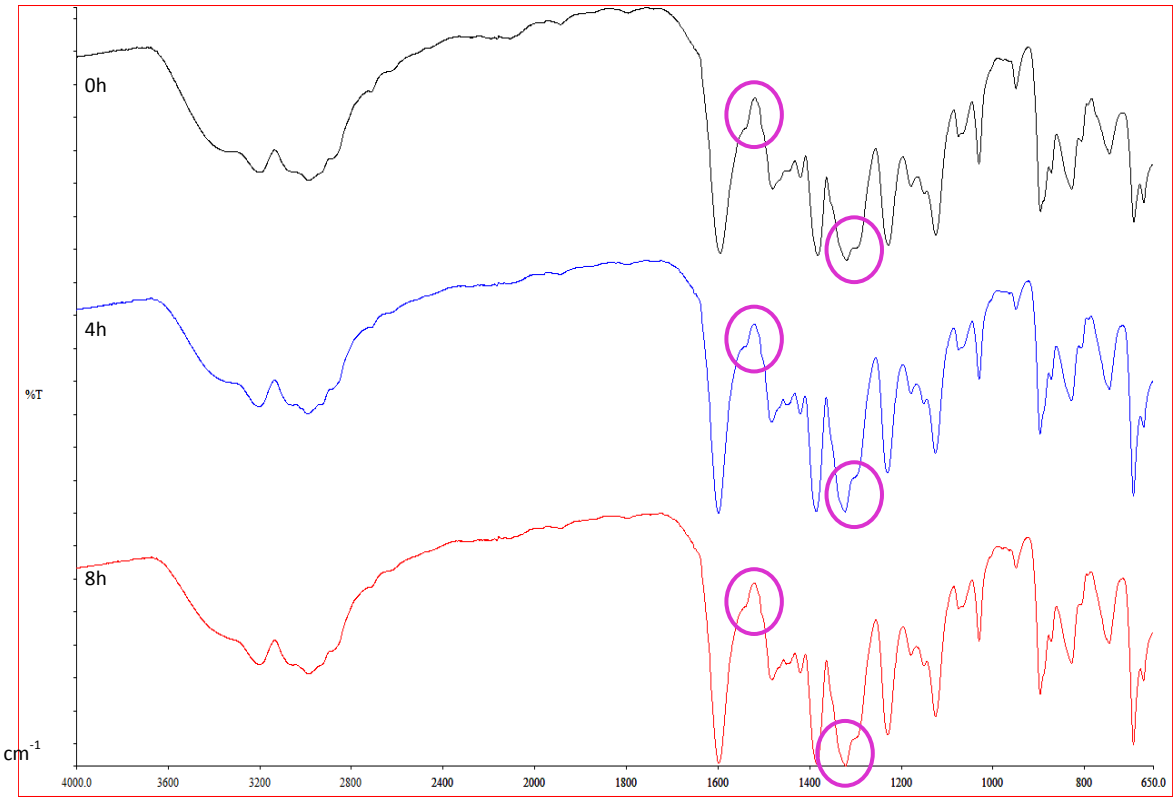

Figure 4.11: Azure A FTIR result

4.4 Tests of dye bound to LAAMScience Fabric

Dyes may have different performances when they are applied to the nonwoven fabric. For this possibility, the dyed fabric photostability is studied in this part through the color change analysis and fabric singlet oxygen producing efficiency tests.

4.4.1 Color CIELAB 76 Test

There is a picture (Figure 4.12) taken from Hunter ColorFlex 45/0 which shows the color difference of the samples from the standard fabric. From left to right, each piece shows one group sample and the upper picture is the background used in this test. This picture indicates the color difference of these samples from visual point.

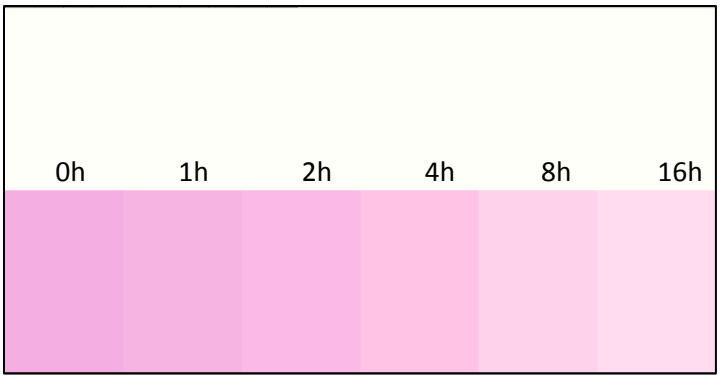

Figure 4.12: Rose Bengal color difference picture

The color analyzed result for Rose Bengal is listed in Table 4.1. It uses the CIE L*a*b* or CIELAB , color scale. The CIELAB color scale is an approximately uniform color scale. It is organized in a cube form. The L* axis runs from top to bottom. The maximum for L* is 100, which represents a perfect reflecting diffuser. The minimum for L* is zero, which represents

black. The a* and b* axes have no specific numerical limits. Positive a* is red. Negative a* is green. Positive b* is yellow. Negative b* is blue.

Table 4.1: Rose Bengal Color CIELAB 76 test analyzed result

Sample ID	L*	a*	b*	ΔE*
Standard	94.51	-1.04	2.96	
0h	75.22	21.78	-12.84	33.81
1h	76.43	20.41	-12.05	31.82
2h	77.48	19.78	-11.09	30.35
4h	79.55	17.18	-9.3	26.57
8h	83.61	12.72	-6.28	19.84
16h	85.82	9.11	-4.06	15.1

Each average of 4 readings consists of an L*, a*, and b* value which corresponds to whether a sample is whiter or blacker (+L*, -L*), redder or greener (+a*, -a*), or yellower or bluer (+b*, -b* respectively). The ΔE* value represents the color difference of the test sample from the standard (non-treated fabric). So there is no ΔE* value for the standard.

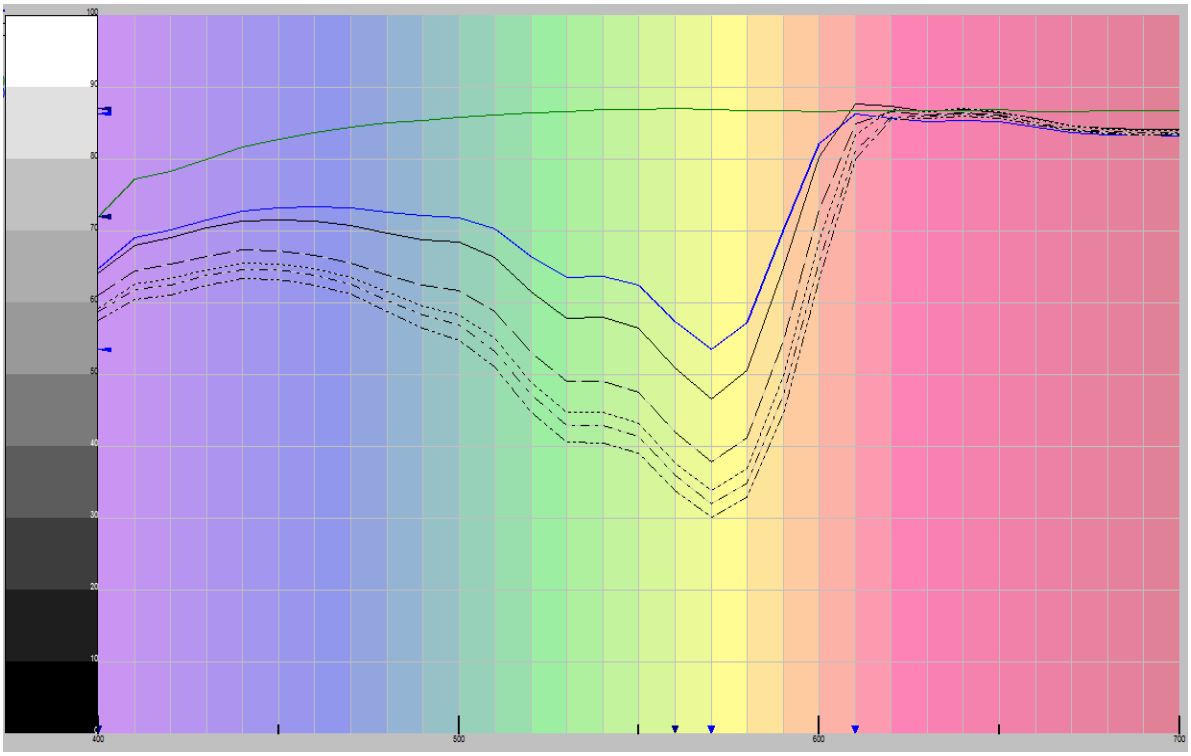

Figure 4.13: Rose Bengal samples color composition chart

By using these data, a color composition chart is obtained as shown in Figure 4.13. From bottom to top are 0, 1, 2, 4, 8, 16 and standard groups separately. From this chart, we can see that all samples are very different from the standard fabric. This color composition shows the color of every sample clearly by describing how white or black, red or green, and blue or yellow they are. Figure 4.14 represents the L*, a*, b* and ΔE* values versus time results. Since ΔE* value is the color difference between test samples and standard fabric, this figure tells us how different every sample is from the standard one from the change of redness, blueness and brightness. L* goes up 12% which is not apparent comparing with redness a* value. a* decreases 58% after 16 hours exposed to solar light. At the same time, b* increases 68%. From 0 hour group to 16 hours group, the ΔE* value keeps falling which refers that the

color is closer and closer to the standard fabric. This is reasonable because the testing samples are photobleached more and more as the exposure time increased.

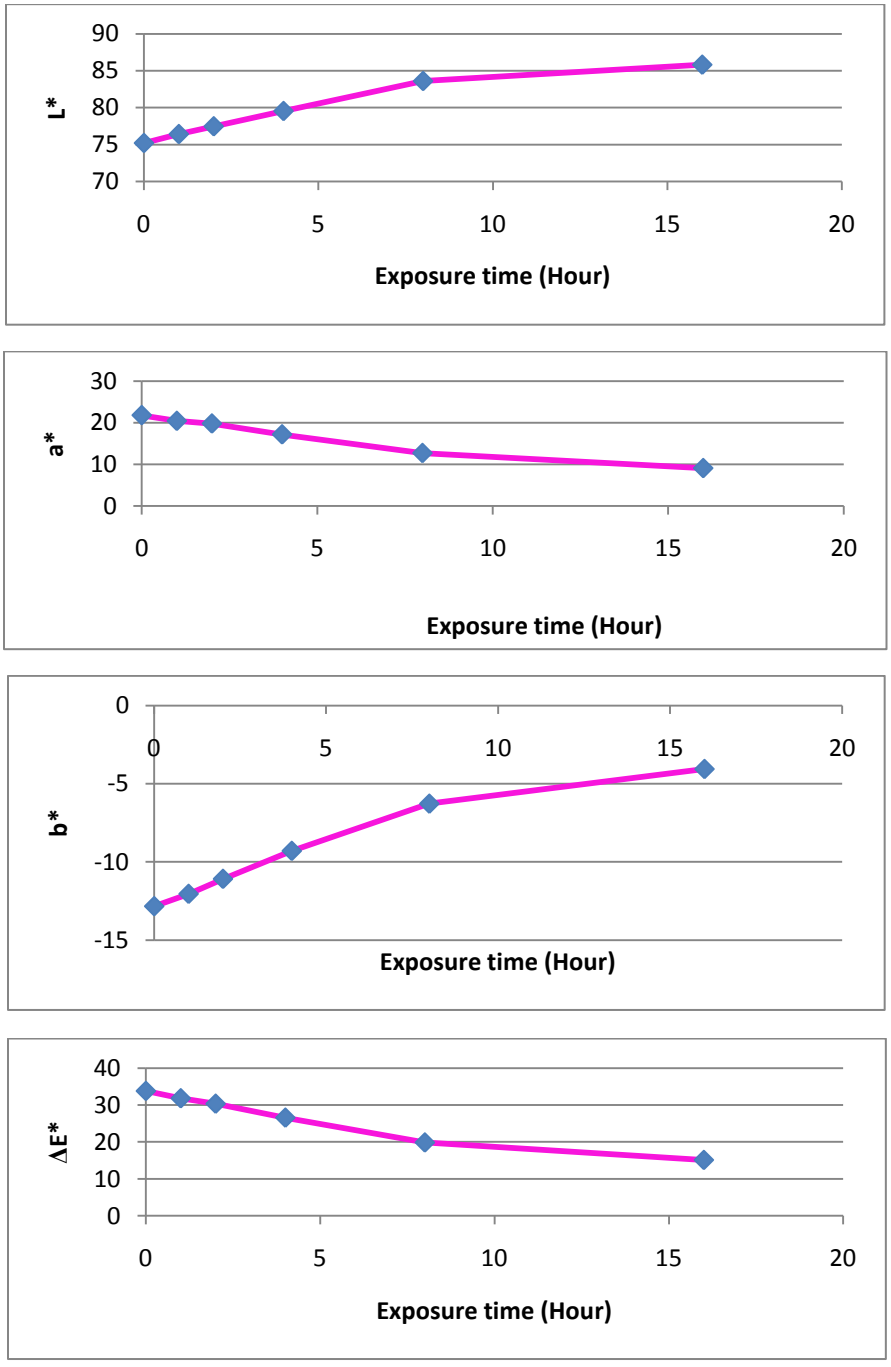

Figure 4.14: Rose Bengal color difference

The same test was done to Azure A dyed fabric. The color result is shown in Table 4.2. And the color difference picture is listed below (Figure 4.15). This result is not as apparent as the Rose Bengal one because the color difference is not that big for Azure A fabric.

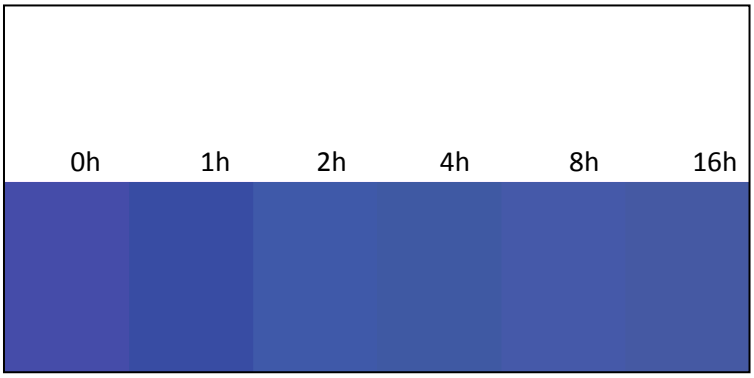

Figure 4.15: Azure A color difference picture

Each piece seems similar but they all show big difference to the standard fabric because the blue color of Azure A on the fabric is darker than pink color of Rose Bengal.

Table 4.2: Azure A Color CIELAB 76 test analyzed result

Sample ID	L*	a*	b*	ΔE*
Standard	94.51	-1.04	2.96	
0h	36.65	7.32	-36.27	70.51
1h	35.65	5.08	-35.36	70.41
2h	38.51	2.40	-33.12	66.71
4h	37.59	1.44	-31.02	66.34
8h	38.94	1.86	-32.40	65.93
16h	39.46	0.59	-30.17	64.27

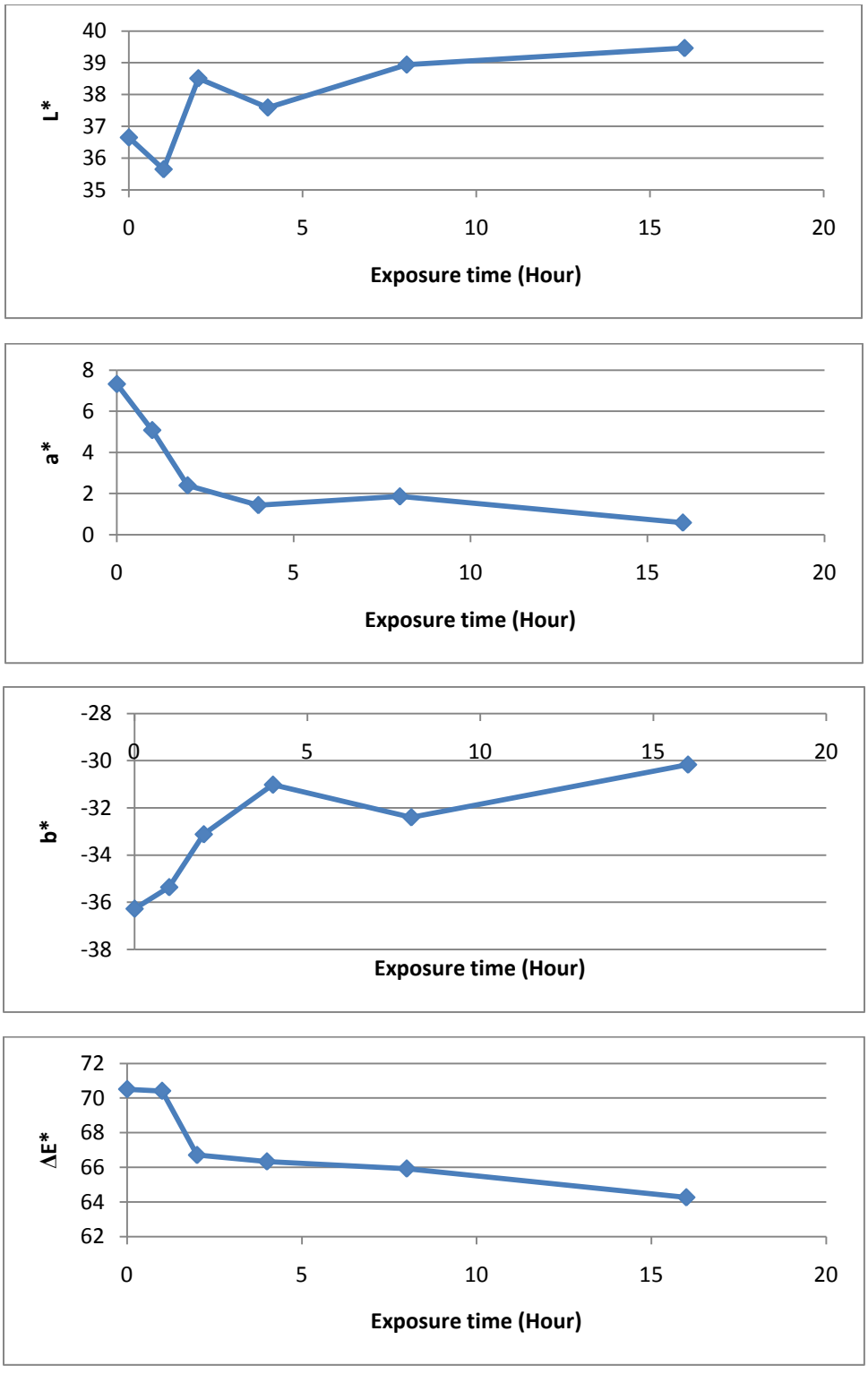

Figure 4.16: Azure A color difference

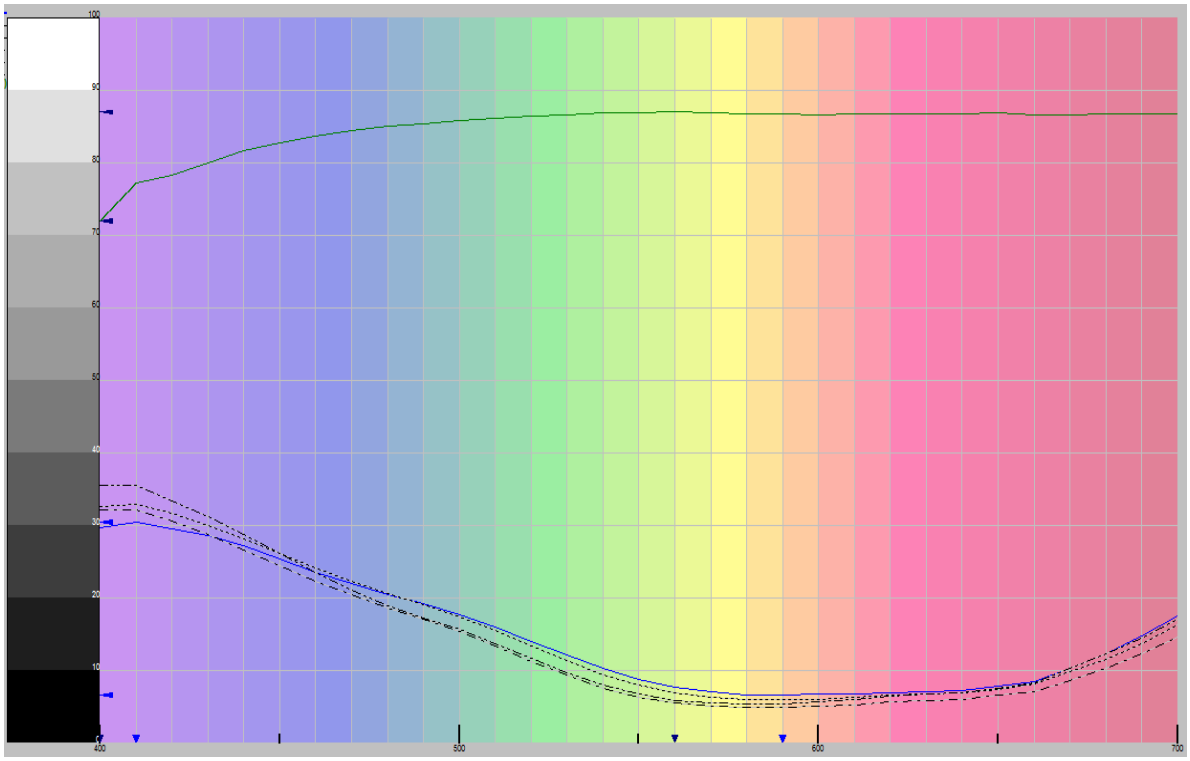

Figure 4.17: Azure A samples color composition chart

ΔE* value in the above table does not fall the same as Rose Bengal. After the first 2 hours, it changes slowly. From Figure 4.16, we can see the trend of L*, a*, b* and ΔE* value versus time results. L* increases 7% finally but there are some bumps before 5 hours. a* keeps decreasing until 8% left for 16 hours group. b* increases 17%. Unlike Rose Bengal, ΔE* value indicates that Azure A falls considerably in the first 2 hours and then changes slowly. This can be also verified by the color composition chart (Figure 4.17).

This chart shows a big difference of the testing samples from the standard fabric but the samples do not show much difference. Azure A may have been fixed better on the fiber surface than the Rose Bengal.

4.4.2 Singlet Oxygen Generation Test

The test system and method are the same as the dye solution samples. And the same analysis was done on the dyed fabrics. The aim of doing this experiment is to study the photostability of the dyes when they are bounded to fabric (on the final product). The test is as complex as the solution, so figuring out the relationship of the efficiency of singlet oxygen generation and the color difference is important. With the research model, simple color test will be applied to the photostability analysis of surface bound dyes which is very meaningful to the industry. Figure 4.18 shows the nylon fabric test result. It also fits the exponential model $A = ae^{-kt}$.

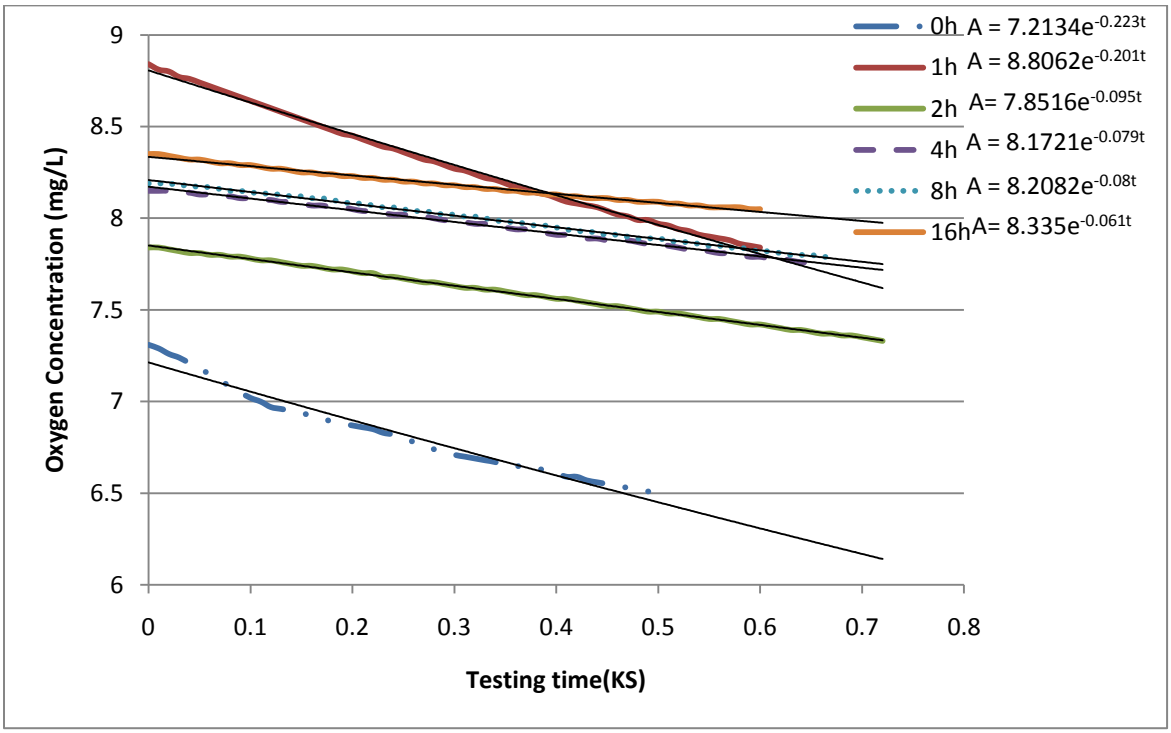

Figure 4.18: Rose Bengal dyed fabric singlet oxygen generation test result

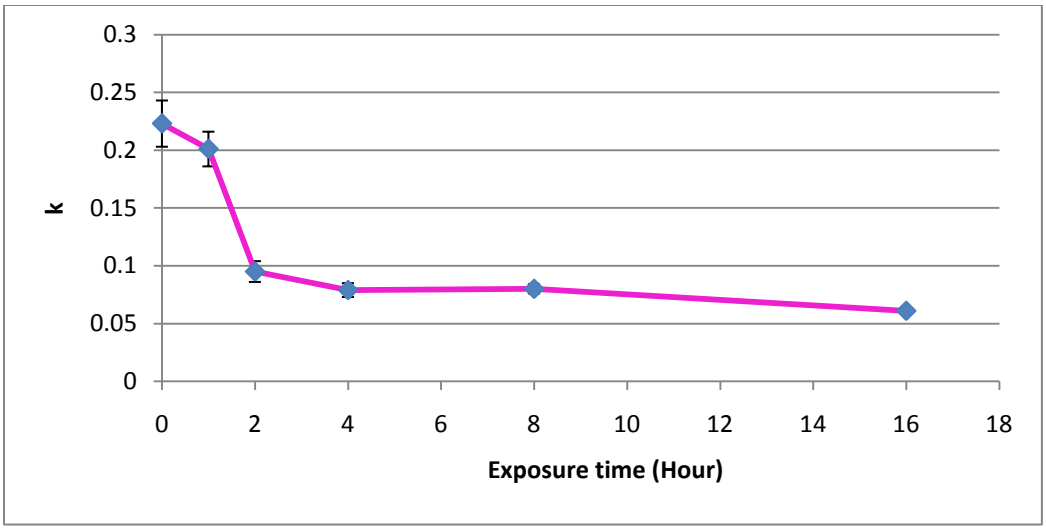

Figure 4.19: k versus time

Figure 4.19 is the rate constant k versus time chart. The k value decreased a lot in the first 2 hours and then decreased slowly afterwards. With the previous color difference parameter analysis result, we can get the relationship of these parameters and k in Figure 4.20, where k is shown plotted versus L*, a*, b* and ΔE* separately. k does not show a high dependence on L* and ΔE* as indicated by the low R square values. But it represents a high correlation to a* and b*.

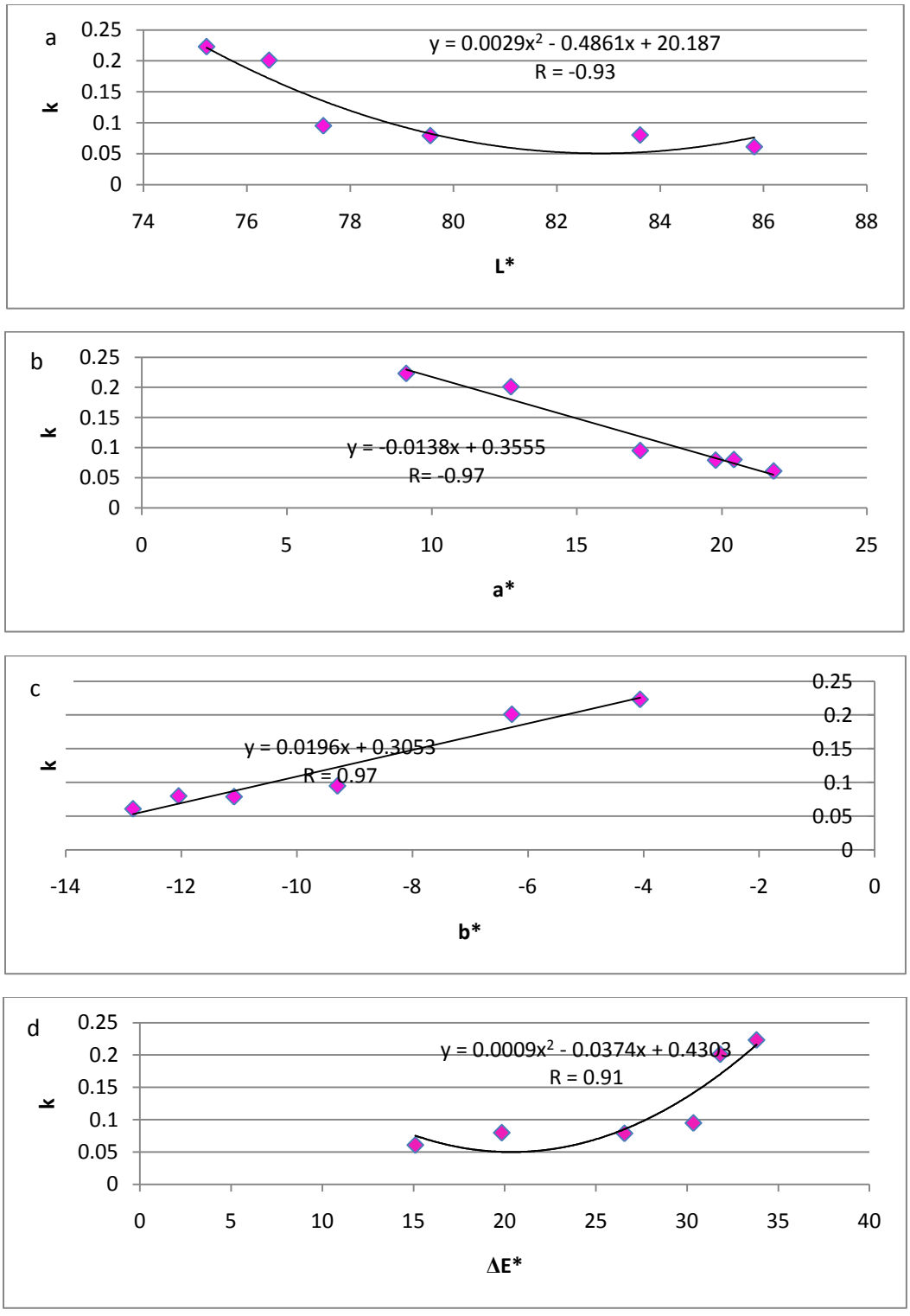

Figure 4.20: The relationship between k and color parameters of Rose Bengal

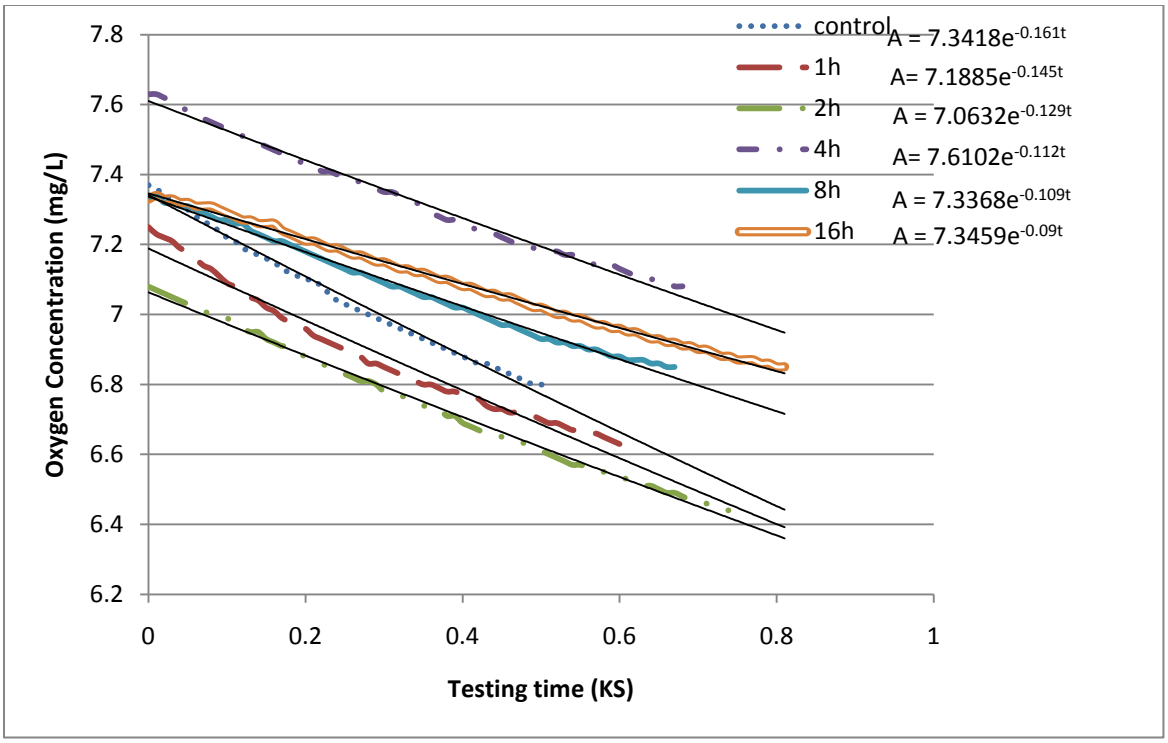

Figure 4.21: Azure A dyed fabric singlet oxygen generation test result

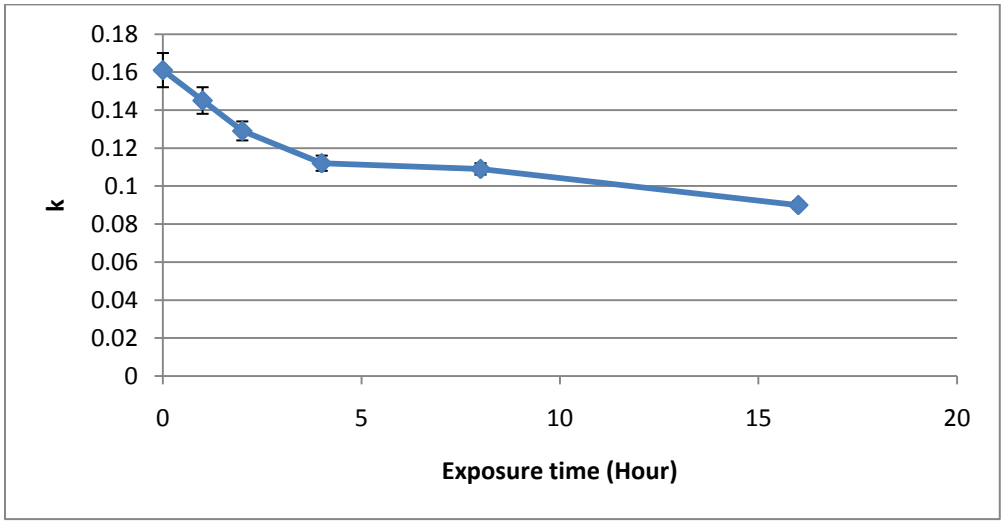

Figure 4.22: k versus time

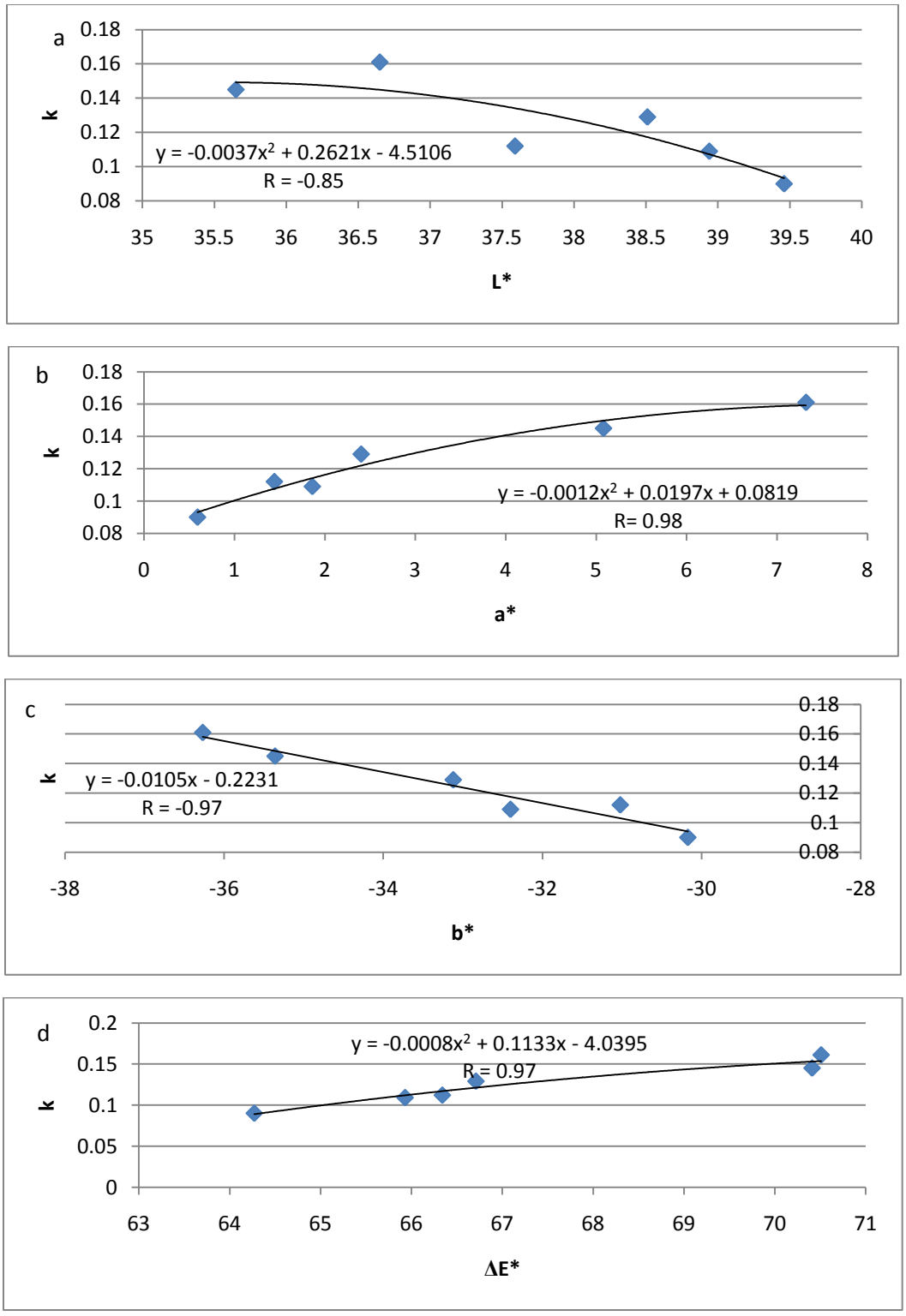

Figure 4.23: The relationship between k and color parameters of Azure A

For Azure A dyed fabric test, similar results were obtained as shown in Figure 4.21-Figure 4.23. Figure 4.21 shows the rate of change the oxygen concentration versus time. The same model was fitted in Azure A case. k versus time chart is shown in Figure 4.22. In this case, k value mainly dropped in the first 2 hours. And comparing with the Rose Bengal dyed fabric, Azure A finished fabric seems more stable. The relationships of k and color parameters are shown in Figure 4.23.

The relationship between k and L* is not meaningful, the relationship between k and a* is better than with ΔE *. So, k and L* are weakly correlated. a* and ΔE * both require a quadratic equation to obtain a good fit with k, while b* is linearly related to k.

4.5 Dyes in different systems

The performances of Rose Bengal and Azure A in different systems are compared. Table 4.3 represents the k value in aqueous and fabric systems for Rose Bengal.

Table 4.3: k values of Rose Bengal in solution and fabric cases

Time (Hour)	k (solution)	k (fabric)
0	1.57	0.223
1	1.22	0.201
2	0.99	0.095
4	0.36	0.079
8	0.24	0.080

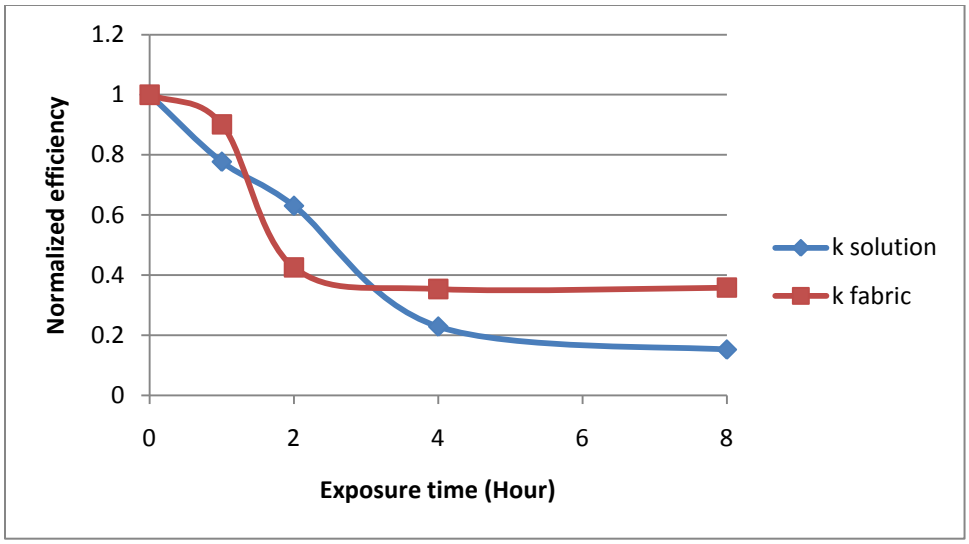

Figure 4.24: Comparison of Rose Bengal in different system

In both systems, k decreases with time. In solution, k decreases 86% while it decreases only 64% in fabric system. And, when it is bound to the fabric, Rose Bengal retains 90% efficiency in the first 1 hour and then begins to lose efficiency more quickly. But in the solution, this value gradually decreases for the first two hours and then decreases faster in the next couple hours. It retains 15% of its singlet oxygen generating ability after 8 hours in solution but 36% on fabric. In general, the fabric system shows better stability for Rose Bengal. The Azure A data is represented in Table 4.4.

Table 4.4: k values of Azure A in solution and fabric cases

Time (Hour)	k (solution)	k (fabric)
0	0.602	0.161
1	0.265	0.145
2	0.255	0.129
4	0.213	0.112
8	0.108	0.109
16	0.069	0.09

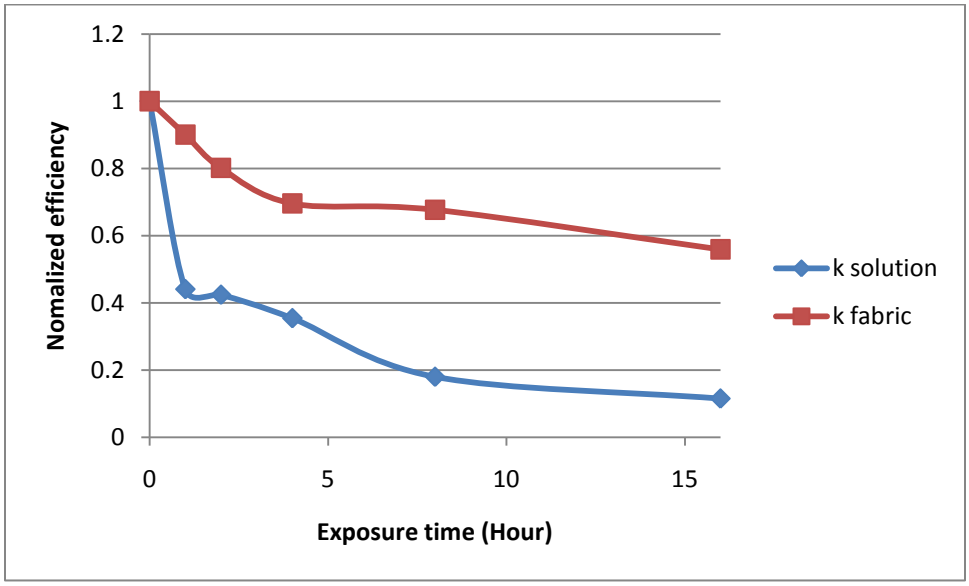

Figure 4.25: Comparison of Azure A in different system

From Figure 4.25, we can see that Azure A shows a very different stability in solution and in fabric system. In solution, k drops rapidly in the first 1 hour and maintains a relatively slow rate change in the following hours. In the fabric system, it keeps a slow drop in rate. The solution system drops 56% efficiency in the first 1 hour while it is only 10% in the fabric case. And it remains 56% efficiency after 16 hours in fabric but only 11% remained in the solution system. Therefore Azure A is much more stable in fabric system than it is in solution system. NH_2 was found changed in the photo-reactions in FTIR. However it is also the bridge of Azure A and nylon polymer. So after being attached to the fabric, this group seems to be more stable.

4.6 Different dyes in the same systems

The absorbance properties of Azure A and Rose Bengal were compared in part 4.1. In the same system, Rose Bengal and Azure A performs different on their stability. Although their initial reaction conditions are different, it seems to be difficult to discuss their difference. We can talk about the change tendencies of them under the same system.

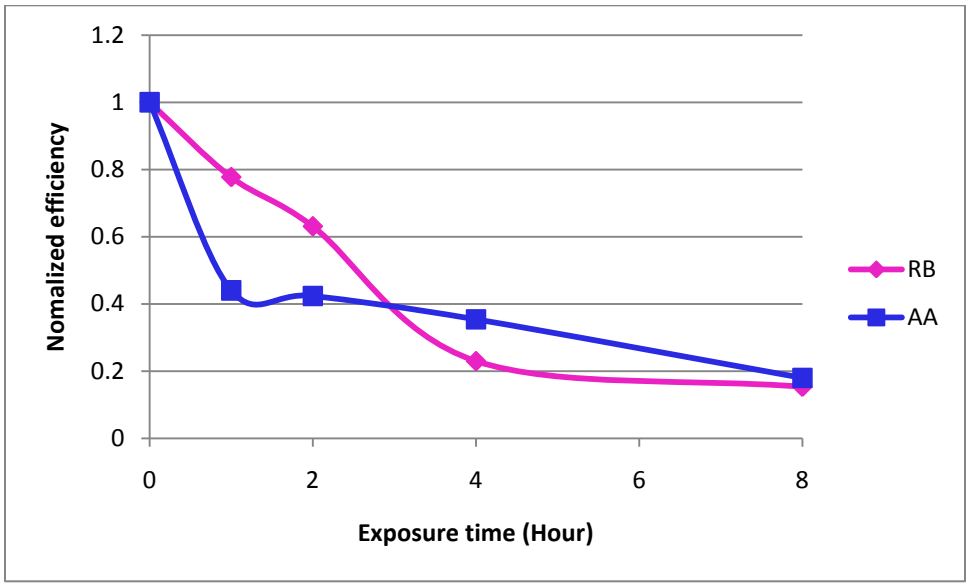

Figure 4.26: k value in solution system for Rose Bengal and Azure A

Figure 4.26 shows the performance of Rose Bengal and Azure A in solution system. As we can see from the above figure, Azure A drops 56% in the first reaction period, which is more than twice as the Rose Bengal (22%). However, after that drop Azure A maintains a slow dropping rate while Rose Bengal keeps dropping faster. After 8 hours, both dyes do not remain much efficiency. The remaining results are 15% and 18% for Rose Bengal and Azure A respectively. So Rose Bengal is better in consistency in the solution condition.

Fabric based comparison is represented in Figure 4.27. Azure A performs a strong stable status in this system. It keeps 56% after 16 hours reaction. Rose Bengal loses much more in this case and only 27% remained after 16 hours. The reason of showing such a result may be there is too much Azure A in the reaction system, or it may be due to the bridge group of Azure A and nylon polymer.

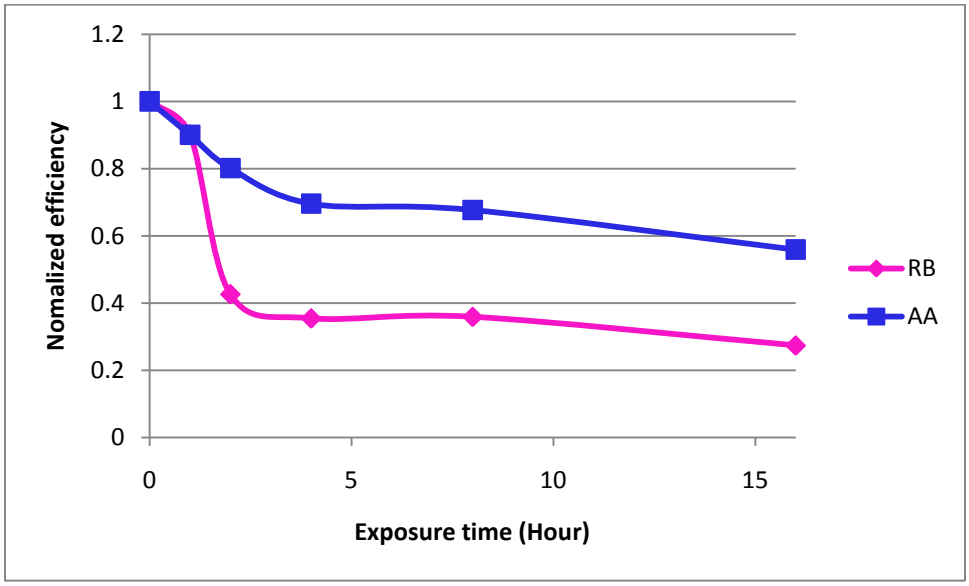

Figure 4.27: k value in fabric system for Rose Bengal and Azure A

5. Conclusions

The photostability of surface bound dyes Rose Bengal and Azure A were studied from several aspects in aqueous system and fabric based system. UV/Vis, FTIR, color test and singlet oxygen generation tests were performed in this research. Several models were used to describe the photostability of these dyes. Comparison between Azure A and Rose Bengal's photostability is discussed in details. Each dye's performances in different systems are compared as well. UV/Vis, FTIR analysis and color test results help in explaining each unique property of both dyes.

In aqueous system, Rose Bengal represents a gradual decrease on the UV/Vis testing result while Azure A drops a lot in the first one hour and then continues to change at a decreasing rate. After 16 hours, Azure A retains only 33% efficiency which is almost inactive in the reaction system. Rose Bengal retains 46% after 8 hours which means it still keeps working. The singlet oxygen generation tests for both dye solutions are very consistent with the UV/Vis result. Both of them fit the exponential model $A = ae^{-kt}$ well. Singlet oxygen producing rate is related to absorbance which is modeled in the linear equation of both dyes. With the simple linear equation, we can skip the complex singlet oxygen generation test. Instead, we can get this information through an easy UV/Vis test. Azure A drops 56% in the first reaction period on the singlet oxygen changing rate k value, which is more than twice as the Rose Bengal (22%). After that drop Azure A maintains a slow dropping rate while Rose Bengal keeps faster drop. After 8 hours, both dyes do not remain much efficiency. The remaining results are 15% and 18% for Rose Bengal and Azure A respectively.

Both FTIR tests indicate some changes on Rose Bengal and Azure A's chemical structures. Rose Bengal was changed on the bond between iodine and benzene ring or the carbon chlorine bond. Azure A's NH_2 was destroyed in the reaction system. This change demonstrates the big difference of Azure A's stability in aqueous system and fabric system. Oxygen is concluded as the most probable reason that lead to these changes because it oxidizes the photosensitizers while it is working.

In the fabric based case, color test result for Rose Bengal dyed fabric is beautifully consistent with the UV/Vis test for Rose Bengal solution while Azure A is totally different on its tendency. The photobleached Rose Bengal dyed fabric samples represent a nicely gradual decreasing ΔE^* value. But Azure A does not change that much. It keeps most of its original color on the fabric. The whiteness and blueness of Azure A only show 7% and 17% change separately. Rose Bengal dyed fabric produces singlet oxygen effectively and the production rate is perfectly linear related to the color parameters a* and b*. Azure A's color test analysis shows that b* is related to the singlet oxygen producing rate linearly, but other parameters are not that meaningful here. On the fabric, Azure A performs a strong stable status. It keeps 56% after 16 hours reaction on the singlet oxygen producing efficiency. Rose Bengal loses much more in this case and only 27% remained after 16 hours. Azure A is much better performed in fabric based system than Rose Bengal.

6. Recommendations for Future Research

All the previous study for this project is helpful to figure out the photostability of surface bound dyes; however there is more work to do in the future. The most important work to be done is to study the effect of the dyes concentration on the photostability of dyed fabrics. Since the current study only focuses on one concentration for each dye. It is difficult to see whether the dye concentration would be an effective factor or not. There is no doubt the dye concentration will affect the absorbance property and fabric color. So it maybe or may not affect the stability of the dyed fabric. An experimentally practical concentration range should be decided for each dye. Then make a group of different concentration samples and test them.

For the purpose of this whole project, it is better to find a best dye. Therefore, apart from Rose Bengal and Azure A, other dyes can be tried too. Although there are some other dyes which were given up for some reasons at the first stage of this study, it is still possible to try something else such as Acridine Yellow G based on the requirements for photosensitizer.

Moreover, mechanism of dye's disappearance should be studied as well. This is another important point because there is not a clear explanation from current references on this issue. A lot of hypothesizes have been proposed by researchers so far. Someone said it is oxidation by oxygen which is essential in this reaction system. And someone else said there is a reduction mechanism. However, no one mechanism has been agreed generally. If one can figure out the unstable reason, something to avoid this process can be done to this material. Maybe more can be done to this system and get the ideal result which means the filtration fabric survives as long as possible under sunlight.

7. References

A. Jodlbauer, H. von Tappeiner. (1905). *Arch Klin. Med., 82*, 520.

A. Soleimani-Gorgani1, J. A. T. (2008). Dyeing of nylon with reactive dyes. part 3: Cationic reactive dyes for nylon. *Dyes and Pigments, 76*, 610-623.

A.U. Khan. (1970). Singlet molecular oxygen from superoxide anion and sensitized fluoresence of organic molecules. *Science, 168*, 476-477.

Alice Maetzke, & Svend J. Knak Jensen. (2006). Reaction paths for production of singlet oxygen from hydrogen peroxide and hypochlorite. *Chemical Physics Letters, 425*, 40-43.

B. W. Henderson, & T. J. Dougherty. (1992). How does photodynamic therapy work? *Photochemistry and Photobiology, 55*(1), 145-157.

B.S. Stowe, V.S. Salvin, R.E. Fornes R.D. Gilbert. (1973). The effect of near-ultraviolet radiation on the morphology of nylon 66. *Textile Research Journal, 43*, 704.

C.A. Rebeiz, K.N. Reddy, O.B. Nadihalli, J. Velu, J. (1990). *Photochemistry and Photobiology, 52*, 1099.

D. C. Neckers. (1989). Review: Rose bengal. *Photochemistry and Photobiology, 47*, 1-29.

D. Wo¨ hrle, A. Hirth, T. Bogdahn-Rai, G. Schnurpfeil, M. Shopova. (1998). *Russ. Chem. Bull., 47*(807)

Eduardo A. Almeida, Sayuri Miyamoto, Glaucia R. Martinez, Marisa H.G. Medeiros, & Paolo Di Mascio. (2003).
Direct evidence of singlet molecular oxygen production in the reaction of acetonitrile with hydrogen peroxide in alkaline solutions. *Analytica Chimica Acta, 482*, 99-104.

Finn Andrew tobiesen, Stephen Michielsen. (2002).
Method for grafting poly(acrylic acid) onto nylon 6,6 using amine end groups on nylon surface. *Polymer Science: Part A: Polymer Chemistry, 40*, 719-728.

Foote, C. S., & S. Wexler. (1964). Singlet oxygen: A probable intermediate in photosensitized autooxidations. *J. Am. Chem. Soc., 86*(3880)

Guoqi Fu , Haiyan Li, Haofeng Yu, Li Liu, Zhi Yuan, Binglin He. (2006).
Synthesis and lipoprotein sorption properties of porous chitosan beads grafted with poly(acrylic acid). *Reactive & Functional Polymers, 66*, 239-246.

He-Hsing Wu, Nini-Chen Tsai,Lie-Hang Shen, Bin Lin, Chia-Chieh Chen, Wuu-Jyh Lin. (2009). *Preparation method for antibacterial nanocomposite fiber materials containing organic intermediates or free-radical scavengers* US 2009/0317434 A1.

Herzberg, G. (Ed.).*Molecular spectra and molecular structure. I. spectra of diatomic molecules. sencond edition*

Huei-Hsiung Wang, C. W. (2005).

Dyeing mechanism and model of nylon 6 fiber dyeing in low-temperature hydrogen Peroxide–Glyoxal redox system. *Wiley InterScience,* doi:10.1002/app.23599

J.E. Baldwin, H.H. Basson, & H. Krauss. (1986). Cleavage of aromatic nuclei with singlet oxygen: Singnificance in biosynthetic processes. *Chem.Commun.,* , 984-985.

J.N. Demas, E.W. Harris, R.P. McBride. (1977). *J. Am. Chem. Soc., 99*(3547)

Jadwiga Buchen Ska. (2001).

Grafting of poly(acrylic acid) on polyamide yarn. *Applied Polymer Science, 80,* 1914-1919.

Krasnovsky, A. A. (1979). Photoluminescence of singlet oxygen in pigment solutions. *Photochemistry and Photobiology, 29,* 29-36.

Lane, N. (2002). Oxygen: The molecule that made the world.

M. A. J. Rodgers, P. Lee. (1984). *Physi. Chem., 88*(3484)

M. Anbar. (1966). Oxidation of molecular nitrogen by excited singlet oxygen molecules in aqueous solution. *J. Am. Chem. Soc., 88,* 5924-5926.

M. Scha¨ fer, C. Schmitz, R. Facius, G. Horneck, B. Milow, K.-H. Funken and J. Ortner. (2000).

Systematic study of parameters influencing the action of rose bengal with visible light

on bacterial cells: Comparison between the biological effect and singlet-oxygen production. *Photochemistry and Photobiology, 71*(5), 514-523.

Martina HavelcovaÂ , Pavel KubaÂ t ,*, Irena NeÏmcovaÂ. (2000). Photophysical properties of thiazine dyes in aqueous solution and in micelles. *Dyes and Pigments, 44*, 49-54.

Milliken, R. S. (1928). Interpretation of the atmospheric oxygen bands; electronic levels of the oxygen. *Nature, 122*, 505.

MM Kamel, Reda M El-Shishtawy, HL Hanna, Nahed SE Ahmed. (2003). Ultrasonic-assisted dyeing: I. nylon dyeability with reactive dyes. *Polymer International, 52*, 373-380. doi:10.1002/pi.1162

N. I. Surovtseva, N. P. Smirnova, A. M. Eremenko, T. V. Fesenko, and V. A. Pokrovsky. (2010). Photodegradation and Aggregation of Acridine Dyes Adsorbed on the Surface of Mesoprorous TiO_2 Films. *Applied Spectroscopy, 77*(2)

N.B. Colthup. (1950). *Optical Soc. Am., 40*, 397.

P. Esser, B. Pohlmann, H.D. Scharf, & Angew. (1994). The Photochemical-synthesis of Fine Chemicals with Sunlight. *Chem., 106*, 2093.

P. Wagler, B. Heller, O. Orther, K.H. Funkn, G. Oehme. (1996). *Chem. Ing. Technol., 68,* 823.

Paolo Di Mascio, Etelvino J.H. Bechara, Marisa H.G. Medeiros, Karlis Briviba, & Helmut Sies. (1994).

Singlet molecular oxygen production in the reaction of peroxynitrite with hydrogen peroxide. *FEBS Letters, 355,* 287-289.

R. Bonnett. (1995). *Chem. Soc. Rev., 19*

R. E. Fornes, R. D. Gilbert, B. S. Stowe, G. P. Cheek. (1973).

Photodegradation of nylon 66 exposed to near-UV radiation. *Textile Research Journal, 43,* 714.

R.C. Allen, R.L. Stjernholm, & R.H. Steele. (1972). Evidence for the generation of an electronic excitation state(s) in human polymorphonuclear leukocytes and its participation in bacterical activity. *Biochem. Biophys. Res. Communi., 47,* 679-684.

R.M. Howes, & R.H. Steele. (1971). Microsomal chemiluminesence induced by NADPH and its relation to lipid peroxidation. *Res. Commun. Chem. Pathol. Pharmocol., 2,* 619-626.

R.V.R. Subramanian, T. V. T. (1972).

Photodegradation of nylon-6. *Textile Research Journal, 42,* 207.

Robert Livngstos. (1947, June).

The Reversible Photobleaching of Dyes and Pigments. *Symposium on Radiation Chemistry and Photochemistry, ,* 24-27.

S. Gavrilyuk,S. Polyutov, P. C. Jha, Z. Rinkevicius, H. Ågren, F. Gel'mukhanov. (2007).

Many-photon dynamics of photobleaching. *Physi. Chem., 111,* 11961-11975.

S. H. Samaha, D. M. Essa, F. M. Tera. (2004).

Acrylonitrile grafting onto nylon-6 fabric. I. synthesis and characterization. *Polymer-Plastics Technology and Engineering, 43*(2), 503-517.

S. N. Gupta, S. M. Linden, A. Wrzyszczynski and D. C. Neckers,. (1988). *Macromolecules, 21*, 52.

S.H. Zeronian, K.W. Alger, S.T. Omaye. (1973).

Effect of sulfur dioxide on the chemical and physical properties of nylon 661. *Textile Research Journal, 43*, 228.

S.M. Burkinshaw, K. Lagonika, D.J. Marfell. (2003).

Sulphur dyes on nylon 6,6—part 1: The effects of temperature and pH on dyeing. *Dyes and Pigments, 56*, 251-259.

Schultz. (1885).

Akademisch verlagsgesellschaft m.b.H.,. In Leipzig (Ed.),

Furbstofftabellen, ()

Siqiang Zhu, Douglas E. Hirt. (2009).

Improving the wettability of deep-groove polypropylene fibers by photografting. *Textile Research Journal, 79*(6), 534-547.

T. Aarthi, Prashanthi Narahari, Giridhar Madras. (2007).

Photocatalytic degradation of azure and sudan dyes using nano TiO2. *Hazardous Materials, 149*, 725-734.

T. Matsuura, A. Nishinaga, N. Yoshimura, & etc. (1969). Photoinduced reactions. I. photooxidative ring-cleavage of dihydric phenols as possible models for biological oxygenation. *Tetrahedron Letters, ,* 1673-1676.

V. S. Srinivasan, D. Podolski, N. Westrick, D. C. Neckers,. (1978). *J. Am. Chem. Soc., 100*(6513)

Vanina Costamagna, Miriamstrumia, Marlo'Pez-Gonza'Lez, Evaristo Riande. (2006).

Gas transport in surface-modified low-density polyethylene films with acrylic acid as a grafting agent. *Wiley InterScience,* doi:10.1002/polb.20945

W.M. Sharman, G.M. Allen, J.E. VanLier,. (1999). *Drug Discov. Today, 4,* 507.

Werner R. Haag, JUrg Hoigne, Ernst Gassman, Andre M. Braun. (1984). Singlet oxygen in surface waters-part I: Furfuryl alcohol as a trapping agent. *Chemosphere, 13,* 631-640.

Zhenzhong Hou, Qun Xu, Qi Peng, Jianbo Li, Haijuan Fan, Shijun Zheng. (2006). Different factors in the supercritical CO2-assisted grafting of poly(acrylic acid) to polypropylene. *Wiley InterScience*, doi:10.1002/app.23857